Quaternary Science Reviews 300 (2023) 107912

Contents lists available at ScienceDirect

Quaternary Science Reviews

journal homepage: www.elsevier.com/locate/quascirev

Deciphering carnivoran competition for animal resources at the 1.46 Ma early Pleistocene site of Barranco León (Orce, Granada, Spain)

Lloyd A. Courtenay [a, b, *], José Yravedra [b, c, d, e], Darío Herranz-Rodrigo [b, c], Juan José Rodríguez-Alba [b], Alexia Serrano-Ramos [f], Verónica Estaca-Gómez [b], Diego González-Aguilera [a], José Antonio Solano [f, g], Juan Manuel Jiménez-Arenas [f, g, h]

[a] Department of Cartographic and Land Engineering, Higher Polytechnic School of Avila, University of Salamanca, Hornos Caleros 50, 05003, Ávila, Spain
[b] Department of Prehistory, Ancient History and Archaeology, Complutense University of Madrid, Prof. Aranguren S/n, 28040, Madrid, Spain
[c] C.A.I. Archaeometry and Archaeological Analysis, Complutense University, Prof. Aranguren S/n, 28040, Madrid, Spain
[d] Grupo de Investigación Ecosistemas Cuaternarios. Complutense University, Prof. Aranguren S/n, 28040, Madrid, Spain
[e] Grupo de Investigación Arqueología Prehistórica. Complutense University, Prof. Aranguren S/n, 28040, Madrid, Spain
[f] Department of Prehistory and Archaeology, University of Granada, Campus Universitario de Cartuja, 18071, Granada, Spain
[g] Museum Primeros Pobladores de Europa 'Josep Gibert', Cam. San Simon, 18858, Orce, Granada, Spain
[h] Institute of Peace and Conflict Research, University of Granada, C/ Rector López Argüeta S/n, 18001, Granada, Spain

ARTICLE INFO

Article history:
Received 12 June 2022
Received in revised form
9 November 2022
Accepted 4 December 2022
Available online 9 December 2022

Handling Editor: Danielle Schreve

Keywords:
Canis mosbachensis
Tooth marks
Trophic pressure
Geometric morphometrics
3D modelling
Computational learning
Archaeological data science
Digital taphonomy

ABSTRACT

Barranco León (Orce, Guadix Baza, Spain) is one of the sites with the oldest evidence of human activity in south-western Europe. This site has yielded human remains in association with both fauna and lithic artefacts, linked through the presence of anthropogenic cut and percussion marks. Nevertheless, while this site is a clear example of early hominin access to carcasses, the accumulations have been identified as a palimpsest, where multiple agents including carnivorans played a role in modifying and interacting in site formation processes. From this perspective, the interpretation and study of the Barranco León site is of great difficulty. Traditionally, interpretations have presented Barranco León as an area where hominins as well as the giant hyena, Pachycrocuta brevirostris, competed for access to carcasses left by machairodontine felids, such as the saber-toothed Homotherium latidens. Nevertheless, as will be presented in this study, the complexity and trophic pressure of Barranco León is much more complicated than originally hypothesized. This study presents a detailed taphonomic analysis of carnivoran activities in the level D1 of the Barranco León assemblage. 3D modelling, geometric morphometrics, and computational learning are used to provide new insights into the tooth pits observed on faunal materials. Here we show that Canis mosbachensis plays a pivotal role in the formation of the site, followed by Pachycrocuta, Homotherium, Ursus etruscus, and Xenocyon (Lycaon) lycaonoides. From this perspective, it can be seen that while Pachycrocuta and Homotherium were active agents in the formation of the site, other carnivorans are also important agents to consider when investigating the Guadix Baza region.

1. Introduction

The Lower Pleistocene of Europe is a key time period that has provided insights into the activity and biology of some of the first hominin populations outside of Africa. Throughout this moment in human evolution, hominins and carnivorans have been documented to have complex relationships, often competing for many of the same resources (Binford, 1981; Brain, 1981; Domínguez-Rodrigo et al., 2007; Rodríguez et al., 2012; Lozano et al., 2016; Rodríguez-Gómez et al., 2016; *inter alia*). In light of the importance of meat consumption in early human evolution, this topic is especially interesting when considering the intensity of this competition for some early European sites and the influence this may have on population dynamics (Périquet et al., 2015), or the basic survival of early *Homo* (Turner, 1992).

One of the most important sites that presents the earliest evidence of this type of competition outside of Africa is the Eurasian

* Corresponding author. Department of Cartographic and Land Engineering, Higher Polytechnic School of Avila, University of Salamanca, Hornos Caleros 50, 05003, Ávila, Spain.
E-mail address: ladc1995@gmail.com (L.A. Courtenay).

https://doi.org/10.1016/j.quascirev.2022.107912
0277-3791/

site of Dmanisi (Tappen et al., 2007, 2022). While sites predating 1 Ma are scarce in Europe, iconic sites such as Pirro Nord (Cheheb et al., 2019), Bois de Riquet (Bourguignon et al., 2016), le Vallonet (Echassoux, 2004), and Sima del Elefante (Huguet et al., 2013), are also fundamental in the study of this topic in early human evolution. Likewise, later Early Pleistocene sites such as Barranc de la Boella (Pineda et al., 2015, 2017), and level TD6 from Gran Dolina (Saladié et al., 2014), are also key case-studies presenting carnivoran-hominin competition. Each of these cases present interesting insights into carnivoran-hominin interactions, ranging from examples of low (e.g. Dmanisi, Bois de Riquet & Barranc de la Boella; *ibid*) to high (e.g. TD6; *ibid*) anthropogenic activity. Other sites such as Le Vallonet and Sima del Elefante (*ibid*), on the other hand, present bones with both carnivoran and anthropogenic cut marks. In either case, both carnivorans and hominins clearly coincided in these sites with the intent of obtaining nutritional resources of some form.

Barranco León (BL, 1.46 Ma, Orce, Guadix Baza, Spain) is another example of an emblematic open-air site from this time period, presenting a clear association between lithic and faunal remains, while yielding one of the oldest hominin fossils in south-western Europe (Toro-Moyano et al., 2013). BL is additionally characterised by an intense exploitation of local flint and limestone raw materials, attributed to the Oldowan techno-complex (Titton et al., 2018, 2020, 2021). Technological analyses have also identified stone raw material exploitation to be concentrated on the production of small flakes in the case of flint, and pounding/percussive activities in the case of limestone (Barsky et al., 2015a; Titton et al., 2018, 2021).

The faunal assemblage of BL presents a diverse range of species in association with human activity, including anthropogenically processed herbivorous large ungulates, such as hippopotamids, equids and cervids, alongside smaller reptiles such as chelonians (Espigares et al., 2019; Yravedra et al., 2022a). Nevertheless, while BL is a site rich with fossil material of archaeological interest, the nature of hominin intervention in this site is still ambiguous, due to the large array of carnivoran activity documented. This palimpsest, alongside other key localities such as Venta Micena (Palmqvist et al., 2002; Luzón et al., 2021), and Fuente Nueva 3 (Espigares et al., 2013; Rodríguez-Gomez et al., 2016; Yravedra et al., 2021), has revealed a great degree of trophic pressure and competition for resources in the region of Guadix Baza. These observations have led authors to construct models with carnivores, such as *Pachycrocuta brevirostris,* as a protagonist in the modification of sites, feasting on the remains of carrion left by other interveners, such as hominins (Espigares et al., 2013), or machairodontine (saber-tooth) felids (Palmqvist et al., 2007a,b, 2011; Rodríguez-Gomez et al., 2016).

Nevertheless, recent taphonomic analyses of the faunal assemblages in this area present contradictory views (Espigares et al., 2019; Yravedra et al., 2021, 2022a), arguing that, at present, insufficient data is available to support these views. These authors argue that the frequency and intensity of carnivoran bite damage is not necessarily analogous with the activity of hyaenids, while the location of cut marks on anatomical elements of higher nutritional value is not an indication of secondary access. In contrast, the frequency of these cut marks does not fit in with models where hominins have primary access to prey (Domínguez-Rodrigo, 1997; Domínguez-Rodrigo, 1999; Domínguez-Rodrigo and Barba, 2006; Domínguez-Rodrigo et al., 2007). From this perspective, the interpretation of BL is still open to debate, while more information is needed in order to truly understand the competition among the multiple agents present in this region.

This study has the objective of performing an in depth analysis on the taphonomic evidence of carnivoran activity in the site of Barranco León, in particular the tooth pits found on bone. The estimation of trophic pressure will play a fundamental role on the interpretation of this site, as data of this nature can provide key insights into the adaptability of early European hominins. Here we support taphonomic finds with the use of 3D modelling, geometric morphometrics, robust statistics, and computational learning in order to present new insights into the bone surface modifications observed on faunal materials. As a result, this study will demonstrate the advantages of using new technological advances to support the interpretation of archaeological and palaeontological sites.

2. The site of Barranco León

The Early Pleistocene site of Barranco León (BL) is found in the northeastern part of the Cenozoic Guadix-Baza Basin (Fig. 1). This area, located in proximity with the town of Orce (Granada, Spain), is rich with archaeological and palaeontological deposits, all of which are crucial for the study of early human evolution. BL is an open air site, consisting of 9 stratigraphic levels (Fig. 1; Anadón et al., 2003; Anadón and Gabás, 2009; Oms et al., 2011), of which levels D1 and D2 are the most relevant in archaeological terms. The present study focuses on the taphonomic analysis of the richest of these layers, level D1 (BL-D1), dated at 1.46 ± 0.19 Ma using Electron Spin Resonance (Toro-Moyano et al., 2013), and in accordance with palaeomagnetic and biostratigraphic data situating this level in the upper Matuyama chron (Oms et al., 2000).

The site of BL is located on the palaeoshoreline of the Guadix-Baza lake. This particular locality has thus been characterised by bordering marginal freshwaters, sourced from the adjacent highlands and mixed with surface and hydrothermal waters from the main saline lake (Anadón et al., 2015). Geologically, BL-D1 is characterised by sandy gravels, product of a sudden event producing high-energy currents (Oms et al., 2011). Palaeoenvironmental data reveal the BL-D1 accumulation to have occurred in a Mediterranean woodland or shrubland environment, yet without an important grassy component (Saarinen et al., 2021), while precipitation and temperature levels would have been higher than in present (Blain et al., 2011, 2016; Sánchez-Bandera et al., 2020; Martínez-Monzón et al., 2021).

The lithic assemblage of BL is mostly comprised of local flint and micritic limestone tools, typical of the Oldowan technocomplex (Turq et al., 1996; Gibert et al., 1998; Toro-Moyano et al., 2009, 2010, 2011, 2013; Barsky et al., 2010, 2015b; Titton et al., 2018, 2020, 2021, *inter alia*), with some quartzite tools as well (Toro-Moyano et al., 2011). These include cores, flakes, flake fragments, debris, retouched pieces, angular fragments, hammers, unmodified cobbles, and subspheroids (Titton et al., 2020). Specialised use of raw materials reveal flint to be preferable for the production of small sharp implements, while limestone is found in the form of percussive devices (Titton et al., 2018). The integrity of the assemblage is highlighted by the presence of refitted artefacts (Toro-Moyano et al., 2013; Titton et al., 2021), additionally highlighting *in situ* knapping processes.

Faunal remains consist mostly of equids, followed by cervids, hippopotamids and bovids (Fig. 2, Supplementary Materials; Espigares et al., 2019; Yravedra et al., 2022a). As for the carnivoran species identified, the BL assemblage contains remains of Hyaenidae such as *Pachycrocuta brevirostris*; Canidae including *Xenocyon (Lycaon) lycaonoides, Canis mosbachensis* and *Vulpes* cf. *alopecoides*; Ursidae including *Ursus etruscus*; Mustelidae including *Meles meles* and *Martellictis ardea* (Ros-Montoya et al., 2021); and finally, the felid cf. *Homotherium* sp. (Martínez-Navarro et al., 2010; Espigares et al., 2019; Yravedra et al., 2022a). While not directly identified in the BL assemblage, BL is also contemporaneous with other large Felidae, including *Megantereron cultridens/whitei*, *Panthera*

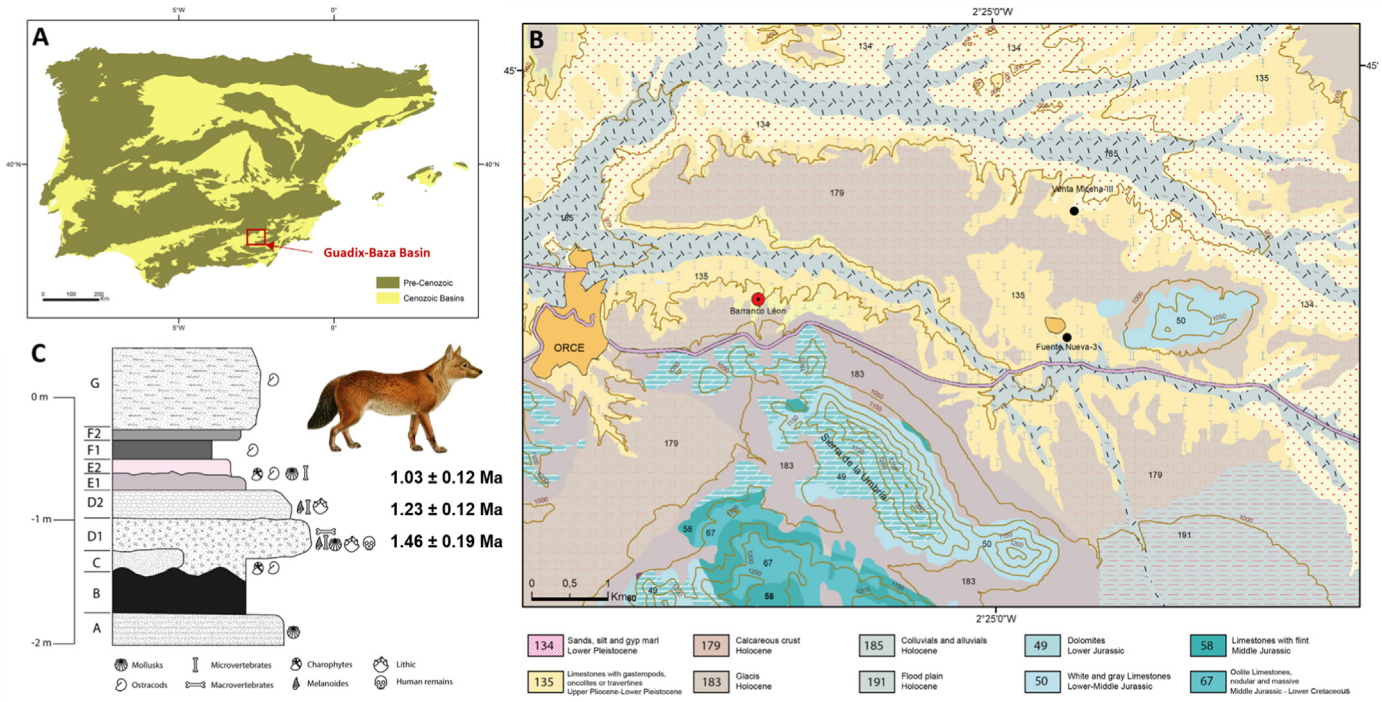

Fig. 1. Location of Barranco León (Guadix-Baza Basin). A. General location of the Guadix-Baza Basin in the Iberian peninsula, B: Regional location of Barranco León in the area around the town of Orce. C: Stratigraphy for Barranco León.

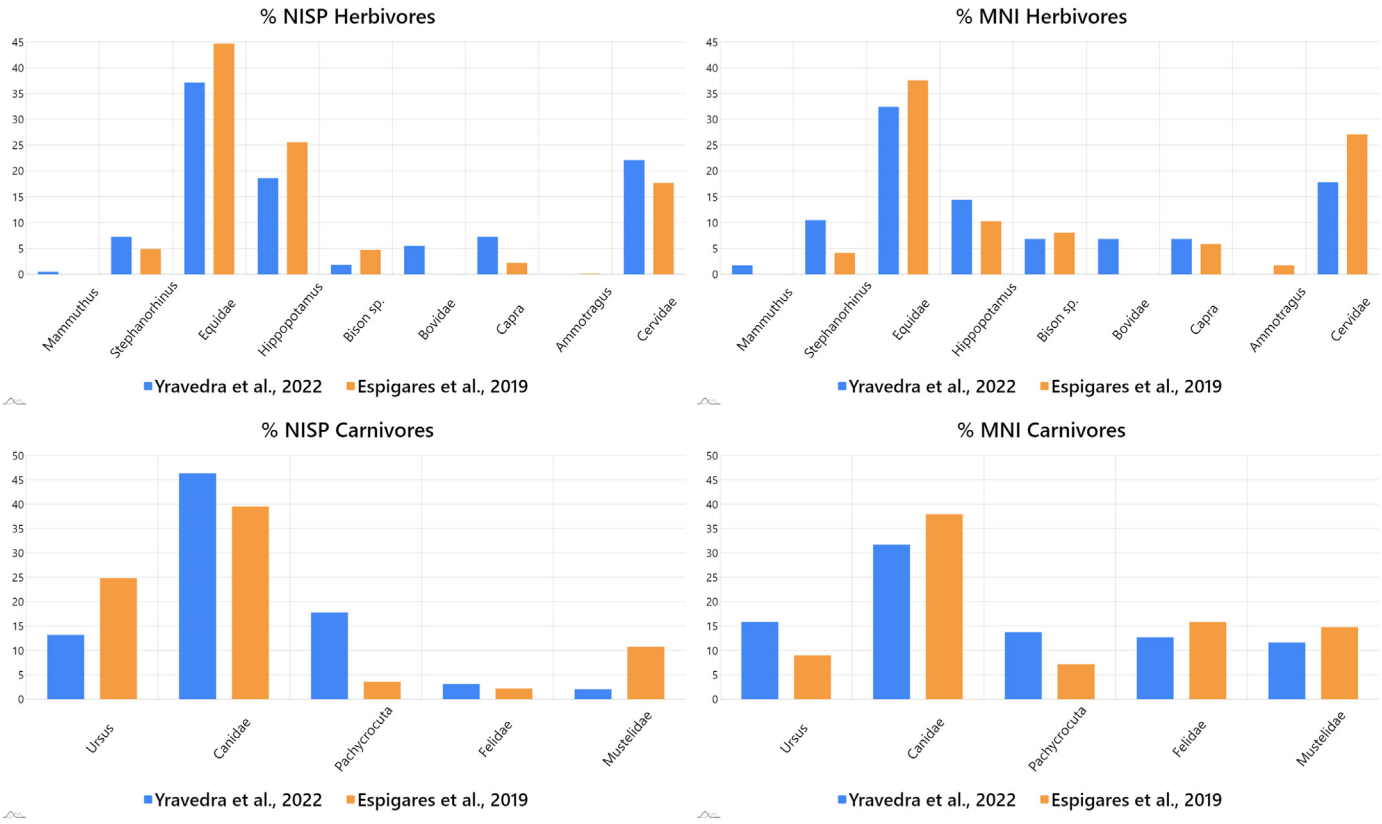

Fig. 2. Taxonomic profiles of BL-D1 calculated by Yravedra et al. (2022a) and Espigares et al. (2019), according to Number of Identifiable Specimens (NISP) and Minimum Number of Individuals (MNI) (See Supplementary Files 1 and 2).

gombaszoegensis and *Acinonyx pardinensis* (Turner, 1992, 1995; Turner and Antón, 1997; Antón, 2013).

Zooarchaeological analyses reveal the BL-D1 assemblage to be mostly composed of adult individuals, with the exception of larger animals (Size 5: 500–1000 kg; Bunn, 1982), who are predominantly represented by non-adult individuals (Supplementary File 2). Skeletal profiles are fully represented, with a predominance of appendicular and cranial elements (Supplementary File 3; Espigares et al., 2019; Yravedra et al., 2022a). Taphonomic data from these remains highlight an intense degree of fragmentation and fractured bones. Cut and percussion marks appear on a wide array of taxa, of all sizes, while carnivoran alterations are intermixed alongside anthropogenic alterations.

Nevertheless, the interpretation of this data is debated by authors, with Yravedra et al. (2022a) proposing carnivorans to have had a more secondary access to faunal remains, as seen through low tooth mark frequencies, as opposed to the primary access proposed by Espigares et al. (2019).

3. Materials and methods

3.1. Sample

The osteological samples obtained from BL-D1 that have been analysed here include 10,848 specimens, excavated between the years 2016 and 2020. The present study thus complements prior zooarchaeological and taphonomic research associated with the levels BL-D1 and BL-D2 (Yravedra et al., 2022a). From this perspective, here we develop a more detailed perspective on the carnivorans who have interacted with the fossil accumulations of BL-D1, and how they may have affected human activities. For the purpose of this study, only bones presenting good cortical surface preservation rates were included, reducing the original sample size to 3559 specimens. Bones were considered to present good cortical preservation if overlying taphonomic processes, such as abrasion or weathering, hindered the ability to inspect cortical surfaces and identify anthropogenic or carnivoran traces (Yravedra, 2005). These specimens were then inspected for the presence of tooth marks.

Tooth marks can be typically categorised into 4 main groups, including (Haynes, 1980, 1983; Binford, 1981; Brain, 1981; Blumenschine, 1995); rounded circular depressions (*pits*), elongated depressions or linear marks with a rounded base (*scores*), circular holes (punctures), and the progressive deletion of bones seen by damage to edges (*furrowing*). The present study has focused the in-depth analysis of tooth marks to only consider tooth pits. This criteria was chosen considering tooth scores to be problematic when including captive carnivorans as a reference sample (Courtenay et al., 2021b), while the use of tooth pits have in general been found to produce higher quality results (*ibid*; Courtenay et al., 2019, 2020a).

Once localised, only entire tooth pits found on the diaphyseal portion of long bones were then separated for digital modelling. This is preferred considering how diaphyses are denser than epiphyses, and are thus more likely to survive both carnivoran feeding as well as taphonomic processes. Carnivorans were fed a number of different sized animals, dependent on the regulations established by the institution where each animal is kept (where applicable). Nevertheless, considering the typical size of prey some of these carnivorans are known to consume, as well as additional data regarding the statistical equivalency of marks on different sized animals, these variables were also considered to be unimportant when selecting tooth pits (Courtenay et al., 2020a, 2021b). Once modified, bones were collected and cleaned in boiling water for 12 h, without the use of additional chemicals.

Fossil materials were cleaned with great care, employing the use of a brush and water solvent, while considering recommendations described by Valtierra et al. (2020).

For the analysis of tooth pit morphologies, the selected fossil tooth marks were then analysed alongside modern comparative materials, consisting of 613 tooth pits originally described and studied by Courtenay et al. (2021a). These include tooth pits by brown bears (*Ursus arctos*, Ursidae, $n = 69$), spotted hyenas (*Crocuta crocuta*, Hyaenidae, $n = 86$), foxes (*Vulpes vulpes*, Canidae, $n = 53$), wolves (*Canis lupus*, Canidae, $n = 80$), African wild dogs (*Lycaon pictus*, Canidae, $n = 89$), leopards (*Panthera pardus*, Felidae, $n = 77$), jaguars (*Panthera onca,* Felidae, $n = 77$), and lions (*Panthera leo,* Felidae, $n = 82$). Samples include tooth pits produced by a mixture of both wild and captive carnivorans. Nevertheless, considering observations made by Courtenay et al. (2020a), captivity is not likely to be a major conditioning factor in tooth pit morphology.

Alongside these modern samples, fossil tooth mark samples attributed to *Pachycrocuta brevirostris,* originating from the Early Pleistocene site of Venta Micena 3 (VM3), were also used for comparative purposes (Yravedra et al., 2022b).

For more details on the modern comparative samples, consult Courtenay et al. (2021a) and their corresponding supplementary materials. For more details on the comparative fossil samples, consult Yravedra et al. (2022a, 2022b).

3.2. Methods

The objectives of the present study are to characterise the interaction of carnivorans with the osteological accumulations found at BL-D1. For this purpose, the present study will be limited only to the description and analysis of carnivoran alterations, including bite damage, fracture planes, as well as digestive alterations. For details on other non-carnivoran related taphonomic processes, consult Yravedra et al. (2022a).

3.2.1. Taphonomic analyses of Carnivoran activity

To characterise the activity of carnivorans in BL-D1, osteological remains were classified and grouped into bones that are taxonomically determinable, or bones that are indeterminable. Wherever possible, indeterminable bones were grouped according to size, following the categories described by Bunn (1982) and Bunn and Pickering (2010). From this perspective, and following the same criteria described by Yravedra et al. (2021, 2022a), fauna were divided into six groups; Microfauna (Size 0), including species weighing less than 25 kg; Very Small Size (1), including macrovertebrates species weighing 25–50 kg; Small Size (2), including species weighing 50–125 kg; Intermediate Size (3), including species weighing 125–500 kg, with an additional division between 3a (125–250 kg) and 3 b (250–500 kg); Large Size (4), including species weighing 500–1000 kg; and Very Large Size (5) for species weighing >1000 kg. Carnivorans were classified according to three separate size classes: small carnivorans (e.g., foxes, lynxes, and mustelids); intermediate carnivorans (e.g., *Canis mosbachensis*); and large carnivorans (e.g., *Homotherium, Megantereon, Ursus* and *Pachycrocuta*), following Espigares et al. (2019).

Bone cortical surfaces were then inspected using 10–40x handheld lenses. Tooth marks were classified either as pits, scores or punctures, while furrowing damage was also analysed (Binford, 1981; Blumenschine, 1995; Blumenschine et al., 1996). Modifications were quantified for specimens with well-preserved bone surfaces, in terms of NISP values.

Once identified, marks were quantified considering their distribution according to anatomic element, while also inspecting the intensity of modifications. This included the calculation of pit-score ratios on long bone diaphyses, which could then be compared with modern day comparative samples described by Arriaza et al. (2019).

Furrowing was also considered following the "taphotype" classes described by Domínguez-Rodrigo et al. (2015), however as this alteration has only been observed on 0.5% of the sample ($n = 18$, Yravedra et al., 2022a), insufficient information is available for an in-depth characterization.

Bone breakage was assessed following the suggestions of multiple authors (Villa and Mahieu, 1991; Alcántara-García et al., 2006; Pickering and Egeland, 2006; Moclán et al., 2019), taking into consideration fracture plane type, metric properties, as well as the presence, absence and type of notch. From this perspective, all green fracture planes were measured using a goniometer (measurement error $\approx 5^{\circ}$), as described by Villa and Mahieu (1991). Notches were then analysed through both descriptive and metric approaches. Considering the current available reference samples for this type of data, only appendicular bones could be used for this analysis, excluding metapodials. Likewise, equids, as well as small (0–2) and large (4 & 5) sized animals had to be excluded. Once data had been collected, these were compared with experimental samples provided by Moclán et al. (2019), which include bones broken by anthropogenic, hyaenid, and canid activities. For this, qualitative and quantitative data were assessed using a Factor Analysis of Mixed Data (FAMD) (Pagès, 2004), followed by the classification approaches described by Moclán et al. (2019). The best performing algorithm obtained for this purpose was the Random Forest (RF; 88.3% Accuracy, Kappa = 0.80).

Finally, when considered necessary, conclusions drawn from zooarchaeological and taphonomic data were supported by complimentary statistical tests. These included tests for equal proportions according to Pearson's χ^2 test statistic, as well as χ^2 contingency table tests. Where tests on contingency tables were found to compute an unreliable test statistic, this test was replaced by the *G* correction of the test statistic (Sokal and Rohlf, 1981).

All statistics were computed using the R v4.0.4 programming language.

3.2.2. 3D modelling and landmark digitization procedures

3D modelling procedures of the selected tooth pits were performed using Structured Light Surface Scanning (Fig. 3). The equipment used was the DAVID SLS-2 located in the C.A.I. Archaeometry and Archaeological lab of the Complutense University of Madrid (Spain). This is a low-cost, powerful, and portable piece of equipment (Maté-González et al., 2017), which could be easily transported to the Museum where fossil materials are located.

Once models had been constructed, tooth pits were digitized using a landmark configuration consisting of 25 landmarks (Fig. 4); five fixed Type II landmarks located on the exterior and interior of each pit, and a 5 × 5 sliding semilandmark patch, removing semilandmarks that overlap with the 5 fixed landmarks (Courtenay et al., 2020b). The 5 fixed landmark are used to mark the maximal length (LM1 & LM2), width (LM3 & LM4), and depth (LM5) of each pit. For the correct orientation of the pit, LM1 is placed farthest away from the perpendicular axis marking the maximal width, and LM2 is thus placed on the opposite extremity. LM3 and LM4 are then placed along this perpendicular axis marking the left (LM3) and right (LM4) maximum extremities. The semilandmark patch is then positioned over the entirety of the pit, so as to capture the internal morphology of the mark and its walls (Fig. 4). Sliding of semilandmarks was performed by minimising

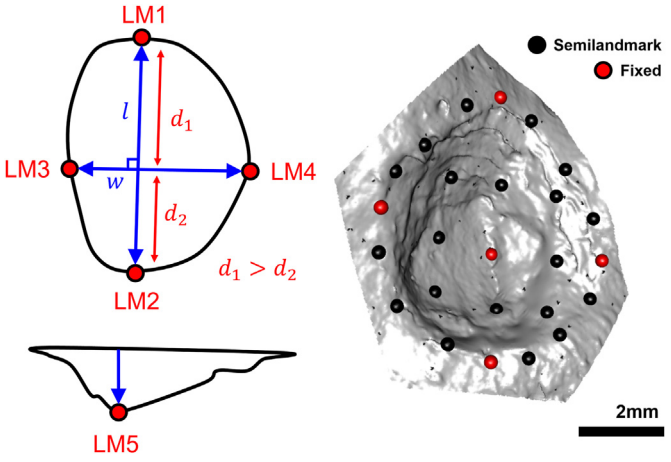

Fig. 4. Detailed graphical description of the landmark model employed. LM = Landmark. w = maximum width. d = distance.

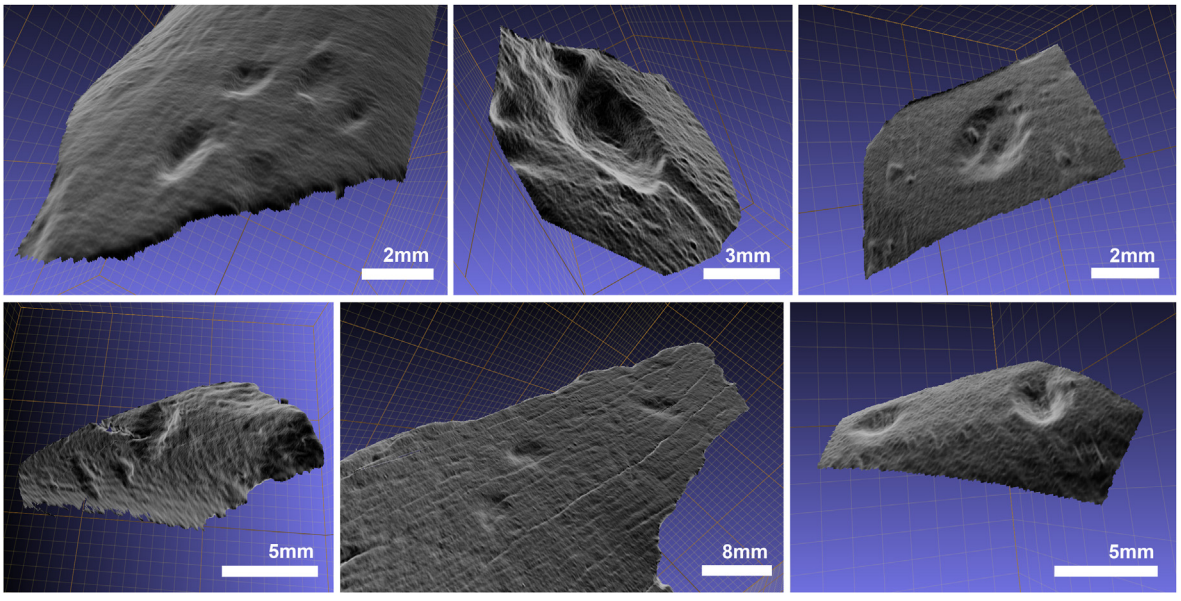

Fig. 3. D models of bite damage produced by carnivorans in the site of Barranco León. 3D models were obtained using Structured Light Surface Scanning.

bending energy based on the Thin Plate Spline (TPS) approach (Bookstein, 1991, 1997; Gunz and Mitteroecker, 2013).

The repeatability of this landmark model was robustly defined as 0.139 ± 0.092 ∈ {0.002:0.586} mm (Courtenay et al., 2020b). These human-induced errors are product of analyst experience, and the time taken to perform the study. All landmarking procedures should thus follow the detailed instructions provided in the main paper and supplementary materials of Courtenay et al. (2020b), while digitization sessions should be performed with as much care and metric accuracy (for defining LM1 to LM5) as possible.

3.2.3. Geometric morphometrics

Once digitized, landmarks were formatted into morphologika files and imported into the R environment (v.4.0.4). Landmarks were first subjected to a Generalized Procrustes Analysis (GPA), so as to normalize data and project landmarks into a new superimposed feature space (Bookstein, 1991; Rohlf, 1999). In order to take into account observations on the weight of tooth pit size (Aramendi et al., 2017; Courtenay et al., 2019, 2021a, b), GPA was performed excluding the scaling procedure, so as to analyse pits in form space. Once superimposed, landmark configurations were analysed in terms of the Procrustes distances between each other, and Centroid Size (CS) distributions.

For Procrustes distances and CS analysis, distributions were first analysed for homogeneity using Shapiro-Wilk tests. All following statistical tests were then conditioned by these results, using traditional statistical approaches where homogeneity was found to be present, and robust statistical approaches otherwise (Höhle and Höhle, 2009; Rodríguez-Martín, 2019; Courtenay et al., 2020b). Descriptive statistics are then calculated considering the mean or median measurement of central tendency (for Gaussian and non-Gaussian data respectively), while distribution variability is measured in terms of the standard deviation or the Median Absolute Deviation (MAD). From a different perspective, univariate statistical tests were also performed, using a linear ANOVA model, or the Kruskal-Wallis test.

Procrustes distance calculations are additionally used to calculate the reference sample with the closest morphological affinity to each of the fossil tooth pits. From this perspective, the original statistical analysis can be used as a first approximation to the classification of each of the tooth pits, which can later be confirmed or fine-tuned using computational learning.

For multivariate analyses, dimensionality reduction via Principal Component Analysis (PCA) was performed. The PC scores representing up to 99% of morphological variance were then selected and used for further statistical processing. Multivariate Analyses of Variance (MANOVA) were used to assess for differences in form feature space, using either the Hotelling-Lawley or Wilk's Lambda test statistic. Finally, Thin Plate Splines (TPS) were also calculated, using a Delaunay 2.5D Triangulation algorithm to facilitate the visualization of landmark configuration patterns (Bookstein, 1989; Lopez-Fernandez et al., 2017).

All statistics were performed in the R (v.4.0.4) programming language.

3.2.4. Computational learning

Once analysed statistically, the observations made calculating morphological affinity with Procrustes distances were then supported by classification algorithms that could provide a final more concrete label to each of the tooth pits.

For the classification of each of the fossil tooth marks, computational learning algorithms were trained, following the procedure recommended by Courtenay et al. (2021a). This methodological workflow consists in (1) the augmentation (x100) of each dataset via an unsupervised approach, followed by (2) the training of supervised classification algorithms (Courtenay and González-Aguilera, 2020; Courtenay et al., 2021a). For data augmentation, a multivariate Monte Carlo Markov Chain was used to simulate the morphological characteristics of 100 tooth marks per sample. This was performed for the balancing of data set sizes, while also preventing over/underfitting in later supervised analyses (Courtenay and González-Aguilera, 2020). Quality of augmented data was then evaluated following the suggestions of Courtenay and González-Aguilera (2020). The final augmented datasets were found to be highly equivalent to the original data ($|d| = 0.004$, $p = 6.9e\text{-}29$).

Once augmented, Support Vector Machines (SVM) and Neural Support Vector Machines (NSVM) were trained (Courtenay et al., 2021a). SVMs were trained using a *k*-fold cross-validated approach ($k = 10$), and a *Radial Basis Function* kernel. Optimal configuration of the kernel was computed using Bayesian Optimisation algorithms (Snoek et al., 2012; Shahriari et al., 2016). NSVMs were trained using typical deep learning approaches (Goodfellow et al., 2016), first employing the use of a Laplacian Random Fourier Function (RFF) -based neural network (Rahimi and Recht, 2007; TancikSrinivasan et al., 2020), and then replacing the final activation layer with a linear SVM (Wieringvan der Ree et al., 2013; Courtenay et al., 2021a). NSVMs were trained in batches of 32 pits for 1000 epochs. The Adam optimizer and a triangular cyclic learning rate were employed. Additional tuning of the SVM activation layer was also performed using Bayesian approaches (Snoek et al., 2012; Shahriari et al., 2016).

Both SVM and NSVM were trained on 80:20% train:test sets, using only augmented data for training. Evaluation was performed on the original dataset. Once trained, algorithms were then used to predict labels and label probabilities for each of the fossil individuals. The summary of the two trained algorithm performance on test sets is provided in Table 1.

SVMs were programmed in the R programming language (v.4.0.4), while NSVMs were programmed in Python (v.3.7.4). For more details see Courtenay et al. (2021a).

Once marks had been classified, fossil tooth pits were separated into their corresponding groups for a more detailed assessment and characterization of the fossil species present. This was performed using the same methodological procedure as the geometric morphometric analyses described above, while additionally testing for morphological equivalence using a Two One-Sided Equivalency tests (TOST), according to Cohen's *d* (Lakens, 2017). For homogeneous distributions, Welch's t-statistic was used, while non-parametric approaches employed the use of Yuen's trimmed robust *t*-statistic.

Finally, TPS were used to calculate mean configurations of different samples, convert these configurations into meshes, and calculate the distance between the faces of each mesh so as to quantify differences between the mean configurations. Distance calculations were computed using the nearest neighbour distance

Table 1
Evaluation results on the trained computational learning algorithms that will be used for the classification of Barranco León tooth marks. SVM = Support Vector Machines. NSVM = Neural SVM. Accuracy, Sensitivity and Specificity are values between 0 and 1, with 1 being the highest obtainab1e value. Kappa values are between 0 and 1, with values above 0.8 being considered a powerful model. Loss considers values closer to 0 as the most accurate models.

	SVM	NSVM
Accuracy	0.93	0.89
Kappa	0.86	0.85
Sensitivity	0.89	0.81
Specificity	0.96	0.96
Loss	0.09	0.10

from a reference mesh to a warped mesh, using as a reference mesh the 3D model corresponding to the median individual of one of the groups (Rohlf, 1998).

3.2.5. Hypothesis testing

In accordance with the recommendations set forth by the editors and contributors of the *American Statistician*, *p*-values were not evaluated using $p < 0.05$ as a threshold for defining statistical significance (Wasserstein et al., 2019), while the term "significant" has also been avoided. In its place, all hypothesis testing was performed using Bayesian calibrations for the evaluation of *p*-values. Under this premise, the False Positive Risk (FPR) was calculated for each *p*-value (Colquhoun, 2019), using the Selle-Berger approach (Benjamin and Berger, 2019) for the definition of Null Hypothesis (H_0) and Alternative Hypothesis (H_a) ratios. Where necessary, FPR was also used to derive Probability of H_0 values ($p(H_0)$), providing a means to calibrate *p* values over 0.3681 (Courtenay et al., 2021a, c). Unless specified otherwise, prior probabilities in support of H_a were set at 0.5, indicating complete randomness, as recommended by Colquhoun (2019).

In light of these calibrations, *p*-values were thus evaluated using a robust value of 0.003 (3σ) as a threshold for more conclusive results. This *p*-value can be considered to have and a FPR of 4.5 +/− [1.2, 15.9] %, using priors of 0.5 +/− [0.2, 0.8] (Courtenay et al., 2021c).

4. Results

4.1. Taphonomic analyses of carnivore activity

Among the 3559 fossils analysed in this study, 368 tooth marks were identified on 167 bones (4.7%) from BL-D1 (Supplementary File 4 & 5). Tooth marks were found on all taxonomic groups and anatomical elements, nevertheless, appendicular long bones were found to present the highest number of tooth marks (Sup. File 5).

The frequency of tooth marks identified are relatively low, with <5% of the osteological sample presenting carnivoran modifications ($\chi^2 = 79.2$, $p = 2.2e\text{-}16$, FPR = 2.2e-12%; Sup. File 4). When considering only appendicular elements, only 74 bones have been observed to present carnivoran bite damage, which is still <20% of the total sample of appendicular elements from BL-D1 ($\chi^2 = 34.8$, $p = 3.6e\text{-}09$, FPR = 1.9e-05%; Sup. File 5 & 6). The intensity of carnivoran damage can additionally be considered low ($\chi^2 = 157.5$, $p = 2.2e\text{-}16$, FPR = 2.2e-12%), when observing 90% of bite marked bones to present less than 5 marks per bone, and no specimen has been observed to present over 10 marks (Sup. File 7). Finally, only 1% of specimens present digestive alterations.

When testing for trends according to animal size, no notable patterns can be observed for neither the presence of bite damage ($G = 2.9$, $p = 0.57$, $p(H_0) = 53.4\%$), nor the frequency of tooth marks per bone ($G = 0.23$, $p = 0.99$, $p(H_0) = 97.4\%$).

Analysing the type of bite damage, punctures are rarely found in BL-D1 ($n = 13$), while pits ($n = 199$) and scores ($n = 156$) are the most common type of tooth mark ($\chi^2 = 231.9$, $p < 2.2e\text{-}16$, FPR <2.2e-12%; Sup. File 7 & 8). When analysing these frequencies in more detail, it can be observed that pits dominate on long bones of animals Size 1, 2 and 3 (pit: score ≈ 59.9 : 40.1%), while larger animals present a predominance of scores (pit: score = 20.0 : 80.0%).

The relationship of pit/score ratios according to animal size has also tested to be of notable importance ($\chi^2 = 16.1$, $p = 0.0003$, FPR = 0.69%). Nevertheless, pit/score ratios have only been found to be important in the case of animal Sizes 4–5 ($\chi^2 = 19.3$, $p = 1.1e\text{-}05$, FPR = 0.03%), while Sizes 1–2 can only be considered to be slightly conclusive ($\chi^2 = 8.3$, $p = 0.004$, FPR = 5.5%). Animals of Size 3 do not present sufficient differences to be considered conclusive ($\chi^2 = 1.1$, $p = 0.30$, FPR = 49.5%). When considering the possible effects that small sample sizes may have on these results, corrected prior probabilities for FPR (priors = 0.2; Courtenay et al., 2021c) still reveal a 2.8% probability that this observation is a false positive in the case of animals of size 4–5. Nevertheless, these corrected priors put into question the reliability of observations made for animals of Sizes 1–2 (FPR = 18.97%). In light of these results, tooth mark frequencies observed on animals of Sizes 4 and 5 can be considered to be similar to those produced by modern day large felids (Domínguez-Rodrigo et al., 2012), nevertheless, score:pit ratios alone are not a diagnostic trait for carnivoran activity, while insufficient data is available to provide a conclusion with regards to smaller animals.

Only a very small sample size of 10 bones (0.3%) were found suitable for fracture pattern analysis. These include a mixture of indeterminable long bone shafts from a mixture of Size 3a and 3 b animals. Among this sample, no epiphyseal regions were found to be present, while the average fragment length was measured at 58.4 mm (Interval 2, according to Moclán et al., 2019). The average number of fracture planes was calculated to be 1, while 70% of this sample present longitudinal fracture planes, followed by oblique fracture planes (30%). Plane angles were mostly measured to be acute ($n = 5$, Circular Mean = 71.6°), followed by obtuse ($n = 3$, Circular Mean = 107.3°). Notches are present on all accounts, varying in number between 1 and 9 notches (average = 3.7), while notch typologies for this sample are mostly incomplete ($n = 6$), followed by simple notches ($n = 2$) and micro-notches ($n = 2$). When performing classifications on these samples, calculations reveal 6 of the bones to have been broken by canids (87.0% confidence), 2 bones to have been broken by anthropogenic agents (74.9% confidence), while 2 bones remain indeterminable (<65% confidence). None of the bones in this sample were found to be product of hyaenid activity. When analysing this data statistically (Fig. 5), the BL-D1 sample is described mostly by low number of fracture planes, small fragment sizes, and mostly acute angles, similar to patterns described multivariately by modern day *Canis lupus*. Nevertheless, this archaeological sample must be increased in future.

4.2. The classification of tooth pits from BL-D1

The BL-D1 tooth mark sample analysed in the present study consist of 64 pits observed on 29 specimens. The majority of tooth pits originate from indeterminable fragments ($n = 11$, 37.9%; Table 2), followed by Size 3 ($n = 9$, 31.0%) and Size 2 animals ($n = 7$, 24.1%). In addition, a single fragment originates from a Size 4 animal (3.4%). Of the 29 bones, only three have been classed as identifiable on a species level, including *Capra alba* (BL19-J48-D1-1), *Equus* sp. (BL20-F47-D1-66), and a single carnivoran individual; *Ursus etruscus* (BL19-F47-D1-29).

The majority of these pits are small (CS Median = 4.4 mm, MAD = 2.6). Robustly calculated 95% confidence intervals ([1.6, 11.8] mm) additionally approximate these samples more in the range of modern wolves (Median = 5.0 mm, MAD = 2.4, 95% CI = [2.8, 9.5]), than any other of the modern comparative samples (Courtenay et al., 2021a). When analysing statistical differences, the BL-D1 sample appears to be more similar to canids of the *Canis* genus ($\chi^2 = 0.2$, $p = 0.7$, $p(H_0) = 57.2\%$), while also revealing some proximities with ursids ($\chi^2 = 2.7$, $p = 0.1$, $p(H_0) = 38.7\%$). Similarly, the majority of the sample is found to be different in size to the tooth pits left by large felids ($\chi^2 = 61.7$, $p = 4.1e\text{-}15$, FPR = 3.7e-13%), followed by Hyaenids ($\chi^2 = 30.19$, $p = 3.9e\text{-}08$, FPR = 1.8e-06%). Nevertheless, the BL-D1 sample presents an inhomogeneous distribution ($w = 0.9$, $p = 0.0002$, FPR = 0.005%), with large variability,

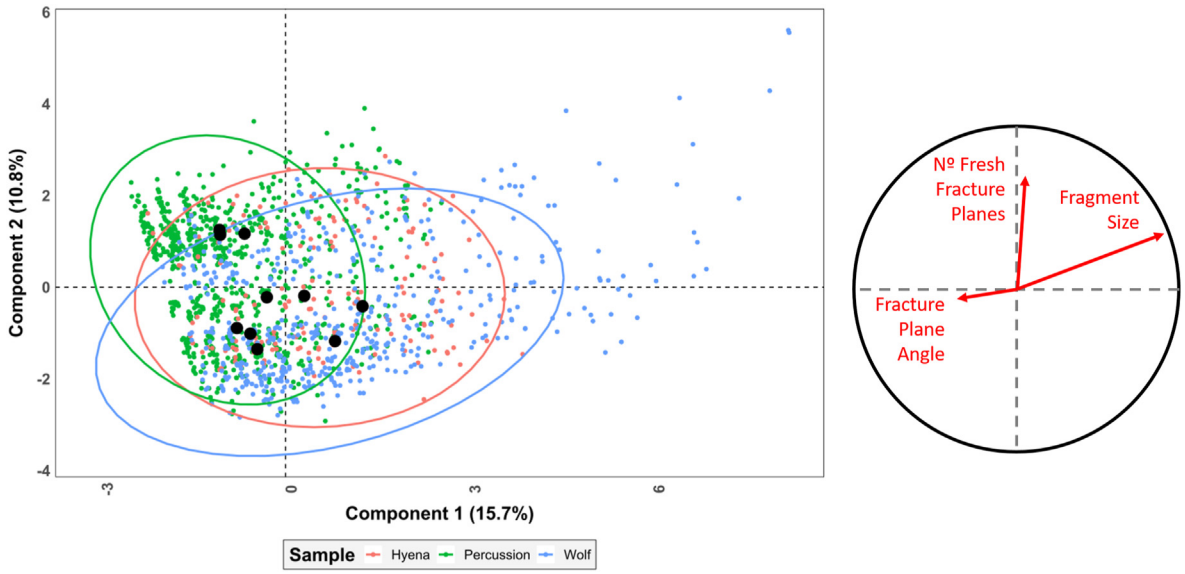

Fig. 5. Factor Analysis of Mixed Data plot of fracture plane variables from modern day carnivore reference samples (Moclán et al., 2019), and the preliminary Barranco León sample (black circles).

indicating the possible intervention of multiple sized carnivorans, with a predominance of smaller animals.

In terms of Procrustes distances, a strong morphological signal can be detected when comparing the entirety of the BL-D1 sample with wolves ($d = 2.5$), with some affinities with ursids ($d = 2.7$). Procrustes distances are greatest when comparing with hyaenids ($d = 3.5$), followed by large felids ($d = 3.3$), while the genus *Lycaon* is also noted to be different ($d = 3.1$).

When combining both morphological and metric variables in form space, the BL-D1 sample exclusively approximates the morphology of modern day *Canis lupus* ($p = 0.45$, $p(H_0) = 50.6\%$), while presenting notable differences with all other samples ($p < 0.001$, FPR <1.8%).

Classifications of the BL-D1 sample using computational learning confirm these observations, with the majority of samples being classed as morphologically similar to modern day *Canis lupus* ($n = 33$, 51.6%). Nevertheless, as indicated by the large mixture of different sized tooth pits, other carnivorans have also been detected, including large members of the Felidae family ($n = 8$, 12.5%), Ursidae ($n = 7$, 10.9%), and Hyaenidae ($n = 6$, 9.4%). Alongside the genus *Canis*, algorithms were able to detect 5 additional canid tooth marks (7.8%), morphologically similar with modern day *Lycaon pictus*.

Finally, a handful of tooth marks were found to be indeterminable ($n = 5$, 7.8%), with both algorithms unable to reach a consensus (probabilities of <70%). Nevertheless, evaluation of these traces reveal them to be much smaller in size than any of the comparative samples (CS mean = 1.9 mm, sd = 0.4, 95% CI = [1.5, 2.3]), with the smallest tooth marks used for comparisons originating from *Vulpes vulpes* (CS mean = 4.1 mm, sd = 1.8, 95% CI = [1.8, 7.8]). From this perspective, it can be hypothesized that these marks originate from a much smaller carnivoran, or an animal capable of producing small tooth pits, not included within the present comparative sample.

When assessing the carnivorans identified according to each fossil specimen, interesting possible interactions between multiple carnivorans can be observed through tooth marks from different species found on the same specimen. This possible competition for resources can be observed in a number of cases, with the tooth marks of both ursids and canids (specimen BL19-K48-D1-172 and BL-14-I52-D1-152), large felids and canids (BL15-F51-D1-45 and BL16-F53-D1-24), large felids and ursids (BL-16-I52-D1-sn and BL17-H56-D1-16), *Lycaon* and Canis (BL18-H47-D1-21), and *Lycaon* and hyaenids (BL19-J48-D1-1), being predicted to have been found on the same bone. Possible competition between canids and hyaenids is also frequent (BL18-L48-D1-71, DL14-I51-D1-26 and DL15-I52-D1-1). The two additional cases of overlap between two species is observed in the presence of smaller tooth pits in association with large carnivorans (BL-15-F50-D1-4 and BL-19-K48-D1-12).

4.3. Characterizing the BL-D1 tooth pit sample

Visualizing morphological variation in accordance with the final classified samples confirms a separation between the predicted species (Fig. 6a), with PC1 (86.53% variance) primarily representing differences in size, and PC2 (1.95% variance) representing variations in shape. Similarly, when comparing the classified fossil samples with the central tendency of their modern day equivalents (Fig. 6b), distributions in form feature space effectively confirm these morphological affinities. From this perspective, each of the detected fossil tooth marks appears to present strong similarities with their modern day relatives (Table 3). In light of this, the suggested *Canis* tooth marks can be associated with *Canis mosbachensis*, the Hyaenidae tooth marks with *Pachycrocuta brevirostris, Lycaon* tooth marks with *Lycaon lycaonoides*, and Ursidae tooth marks with *Ursus etruscus*. While some overlap still exists between samples seen through some equifinality in form Procrustes distances, general trends in multivariate feature space seem to separate *Canis* individuals from both Ursidae, Hyaenidae, and *Licaon*, while Felidae samples are restricted to one extreme of feature space. The smaller size of the BL-D1 *Canis* tooth marks also create some morphological affinities with modern day *Vulpes vulpes*, however this point will be explored in further detail in the following section.

In the case of Felidae, the tooth pits from the present sample are slightly smaller than that of the modern day *Panthera leo* (Table 4; Fig. 7), however larger than both that of *Panthera pardus* and *Panthera onca*. Similarly, morphological data reveals the felid tooth pits at BL-D1 to be closer in form to *Panthera leo* (Table 3), while

Table 2
Classification results, Procrustes Form Distances (Proc. D), and Centroid Sizes, for each of the Barranco León tooth marks analysed in the present study. Sp. ID indicates the Specimen's ID (Site-Year-Square-Level-Number). Where possible, animal size classes have been included. Procrustes distances are calculated from each pit to their corresponding classified label. Computational Learning (CL) classification percentages are obtained from the most confident classification algorithm (Support Vector Machines (SVM) or Neural Support Vector Machines (NSVM).

Sp. ID	Size	Class Label	Proc. D	CL Probability	Algorithm	Centroid Size
BL-14-G49-D1-105	Indet	Felidae	2.47	83.07%	SVM	11.77
		Felidae	1.92	83.05%	SVM	10.14
Sn	3 b	*Lycaon*	0.9	93.12%	SVM	6.72
		Lycaon	1.32	86.54%	SVM	6.26
BL-14-F52-D1-116	Indet	*Canis*	1.08	75.96%	SVM	3.47
		Canis	1.54	95.61%	SVM	2.98
		Canis	1.14	82.30%	SVM	5.01
BL-14-I52-D1-152	Indet	*Canis*	0.29	100.00%	SVM	4.46
		Ursidae	1.06	79.06%	SVM	5.89
		Ursidae	1.24	89.83%	SVM	5.49
Sn	4	Felidae	2.85	85.37%	SVM	12.46
BL-16-F53-D1-24	3	*Canis*	2.98	96.05%	SVM	1.48
		Canis	2.86	97.39%	SVM	1.61
		Canis	1.44	99.16%	NSVM	5.27
		Felidae	1.95	88.31%	SVM	11.77
BL-14-I51-D1-26	3a	Hyaenidae	0.56	82.65%	NSVM	5.1
		Canis	0.96	74.64%	NSVM	4.33
BL-15-I52-D1-1	3	Hyaenidae	1.8	85.24%	SVM	7.96
		Canis	1.25	81.07%	SVM	3.73
BL-15-F50-D1-4	Indet	*Canis*	1.68	89.67%	SVM	2.7
		Indet				1.9
BL-15-G51-D1-22	Indet	Indet				1.63
BL-15-F50-D1-46	Indet	*Canis*	1.37	85.01%	NSVM	3.69
BL-15-F51-D1-45	Indet	Felidae	2.37	90.45%	SVM	8.99
		Canis	1.45	90.78%	NSVM	3.05
		Canis	2.86	75.95%	SVM	5.9
		Felidae	1.3	81.69%	SVM	8.32
BL-17-H56-D1-16	2	Ursidae	0.70	98.96%	NSVM	7.34
		Ursidae	1	89.55%	NSVM	4.97
		Felidae	2.66	85.37%	SVM	10.51
BL-17-F48-D1-22	Indet	*Canis*	2.59	87.05%	SVM	1.88
		Canis	2.08	77.96%	NSVM	2.39
BL-17-I48-D1-200	Indet	*Canis*	1.68	97.39%	SVM	2.83
BL-18-J48-D1-10	3 b	*Canis*	0.79	94.51%	NSVM	4.12
		Canis	1.1	91.44%	NSVM	2.3
		Canis	2.16	90.28%	NSVM	2.1
BL-18-L48-D1-71	2	Hyaenidae	1.68	75.15%	NSVM	6.97
		Hyaenidae	2.17	98.29%	NSVM	9.2
		Canis	1.16	80.56%	SVM	3.47
		Canis	0.94	100.00%	SVM	3.63
BL-18-J48-D1-144	2	*Canis*	0.98	97.07%	SVM	3.64
BL-18-H47-D1-21	3	*Canis*	0.8	100.00%	SVM	4.44
		Canis	1.63	80.67%	NSVM	2.92
		Lycaon	1.16	85.65%	NSVM	6.01
BL-18-K48-D1-223	2	*Canis*	1.04	98.79%	SVM	3.49
		Canis	0.88	80.84%	SVM	3.77
BL-19-J48-D1-1	2	*Lycaon*	1.10	83.44%	SVM	7.12
		Lycaon	1	90.48%	NSVM	5.62
		Hyaenidae	1.58	87.81%	NSVM	8.06
BL-19-L48-D1-15	2	*Canis*	1.16	84.22%	NSVM	4.24
BL-19-K48-D1-12	Indet	Indet				2.33
		Indet				2.15
		Indet				1.47
		Canis	1.04	84.27%	SVM	3.6
BL-19-K48-D1-172	2	*Canis*	2.66	86.30%	NSVM	1.8
		Canis	1.67	85.50%	NSVM	2.82
		Canis	2.52	85.17%	NSVM	1.98
		Ursidae	0.84	83.92%	NSVM	6.85
BL-19-F47-D1-29	Carn3	Hyaenidae	1.55	79.55%	NSVM	6.17
BL-20-F47-D1-11	3	Ursidae	1.40	90.30%	SVM	5.2
BL-20-F47-D1-26	3 b	*Canis*	0.43	91.81%	SVM	4.37
BL-20-L48-D1-99	3 b	*Canis*	0.49	93.01%	SVM	4.21
BL-16-I52-D1-sn	Indet	Felidae	1.62	87.08%	SVM	12.09
		Ursidae	1.14	89.40%	NSVM	6.51

Procrustes distances are much greater when compared with both other species of felid. From this perspective, and using *Homotherium latidens* as the closest analogy with *Panthera leo* in size (Turner and Antón, 1997; Antón et al., 2005, 2014; Antón, 2013), the BL-D1 sample can therefore be approximated to *H. latidens*, as opposed to the smaller *Megantereon cultridens,* and *Panthera gombaszoegensis*, which are more similar to the modern day *Panthera onca*.

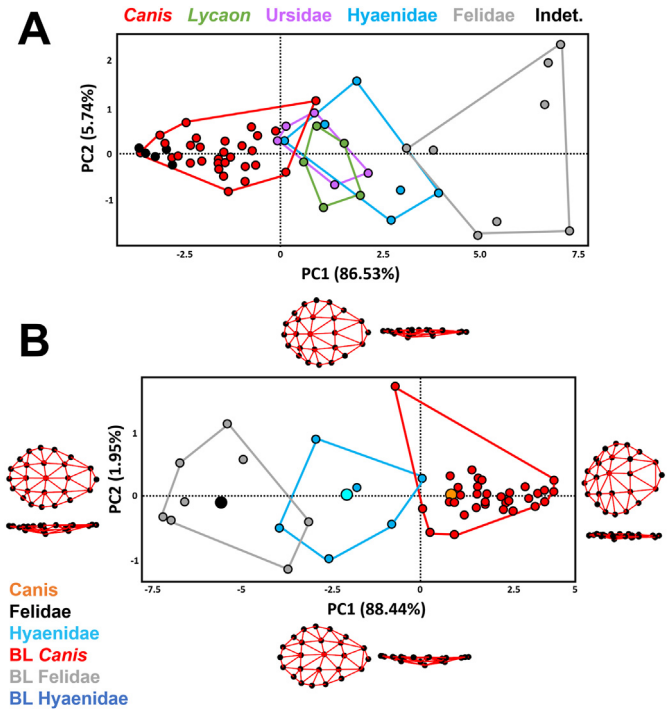

Fig. 6. – Principal Component Analyses (PCA) in Form feature space characterizing (A) the morphological variation of each of the BL-D1 samples, and (B) the mean PCA comparing modern day carnivoran central configurations with each of the main BL-D1 samples. For the purpose of visual clarity, ursids, Lycaon and any indeterminable marks have been excluded from panel B. Predicted form deformations via thin plate splines are depicted on each extremity of their corresponding PC score in panel B, employing the use of a 2.5D Triangulation algorithm.

4.4. Characterising fossil carnivorans from orce

Due to the smaller sample sizes of fossil *Homotherium latidens* and *Ursus etruscus* tooth pits, the detailed characterization of the fossil tooth pits will focus solely on the analysis of suggested Canidae from BL-D1, as well as predicted Hyaenidae tooth marks combining data from BL-D1 and VM3 (Yravedra et al., 2022b).

4.4.1. Canis mosbachensis

The sample classed as *Canis mosbachensis* is very similar to the comparative samples produced by modern day *Canis lupus*, presenting noticeable overlap in form feature space (Fig. 8). Based on this data, morphologically speaking *Canis mosbachensis* can be described by presenting mostly superficial pits. This links strongly with observations made on *Canis lupus* specimens by multiple authors (Yravedra et al., 2019; Courtenay et al., 2020a, 2021a, b). When compared in general with other large canids, both species of *Canis* are restricted to a portion of feature space described by more asymmetrical pits, with the point of maximal depth shifting closer to one edge of the pit than the other (PC1 = 87.02% variance). The predicted *Lycaon* samples, on the other hand, are observed to be much deeper, with a greater variance across feature space, while their tooth pits are observed to be more elongated, with the point of maximal depth shifting along the LM1-LM2 axis.

When considering size, allometry is present between *Lycaon* and *Canis* samples ($F = 22.3$, Residuals$^2 = 0.027$, Effect Size (ES) = 5.7, $p = 0.001$, FPR = 1.8%), as well as between *Canis lupus* and *Canis mosbachensis* ($F = 19.0$, Res.$^2 = 0.030$, ES = 0.3, $p = 0.001$, FPR = 1.8%). Allometry between *Canis mosbachensis* and *Vulpes vulpes* is much less evident ($F = 2.72$, Res$^2 = 0.008$, ES = 2.1, $p = 0.02$, FPR = 19.1%). These observations indicate size to be a conditioning factor in the morphological variation between most

Table 3
Procrustes distances calculated in form associating the final classified fossil species from BL-D1 with their extant relatives. *Including only BL-D1 fossil specimens. **Including both BL-D1 and VM3 fossil specimens.

	C. lupus	L. pictus	C. crocuta	U. arctos	*P. leo*	P. onca	P. pardus	V. vulpes
C. mosbachensis	1.233	3.641	4.387	2.595	8.074	3.943	0.993	0.255
L. lycaonoides	2.302	0.799	1.321	1.312	4.749	1.149	2.606	3.470
*P. brevirostris**	1.282	1.270	2.433	0.641	5.676	1.572	1.523	2.433
*P. brevirostris***	1.005	1.592	2.329	0.692	5.992	1.869	1.203	2.124
U. etruscus	2.173	0.790	1.418	0.908	4.884	0.948	2.378	3.319
H. latidens	7.160	4.806	4.054	5.847	1.125	4.514	7.415	8.336

Table 4
Descriptive statistics comparing centroid sizes of each of the samples analysed within this study. *Samples from Barranco León. **Samples from Barranco León and Venta Micena 3 (Yravedra et al., 2022b). Lower and Upper Confidence Intervals (CI) are calculated using robust 95% quantile intervals.

		Min	Lower CI	Central	Deviation	Upper CI	Max
Canidae	*Lycaon pictus*	2.23	3.13	6.65	3.06	17.24	22.09
	*Lycaon lycaonoides**	5.76	5.76	6.44	0.56	7.19	7.19
	Canis lupus	2.14	2.52	4.56	2.18	8.59	14.18
	*Canis mosbachensis**	1.49	1.62	3.45	1.15	5.42	6.49
	Vulpes vulpes	1.10	1.73	3.74	1.63	7.02	7.49
Felidae	*Panthera leo*	3.90	4.52	11.00	6.00	24.67	31.51
	*Homotherium latidens**	8.34	8.34	10.92	1.56	12.64	12.64
	Panthera onca	1.68	2.55	6.94	3.86	19.42	28.90
	Panthera pardus	2.44	2.67	4.40	1.92	8.53	10.65
Hyaenidae	*Crocuta crocuta*	2.62	3.50	7.38	3.21	15.93	23.64
	*Pachycrocuta brevirostris***	2.49	2.57	5.40	2.54	12.16	14.93
Ursidae	*Ursus arctos*	1.54	1.63	5.87	3.67	12.69	16.90
	*Ursus etruscus**	4.99	4.99	6.11	0.86	7.37	7.37
BL-D1 Indeterminable		1.48	1.48	1.92	0.36	2.36	2.36

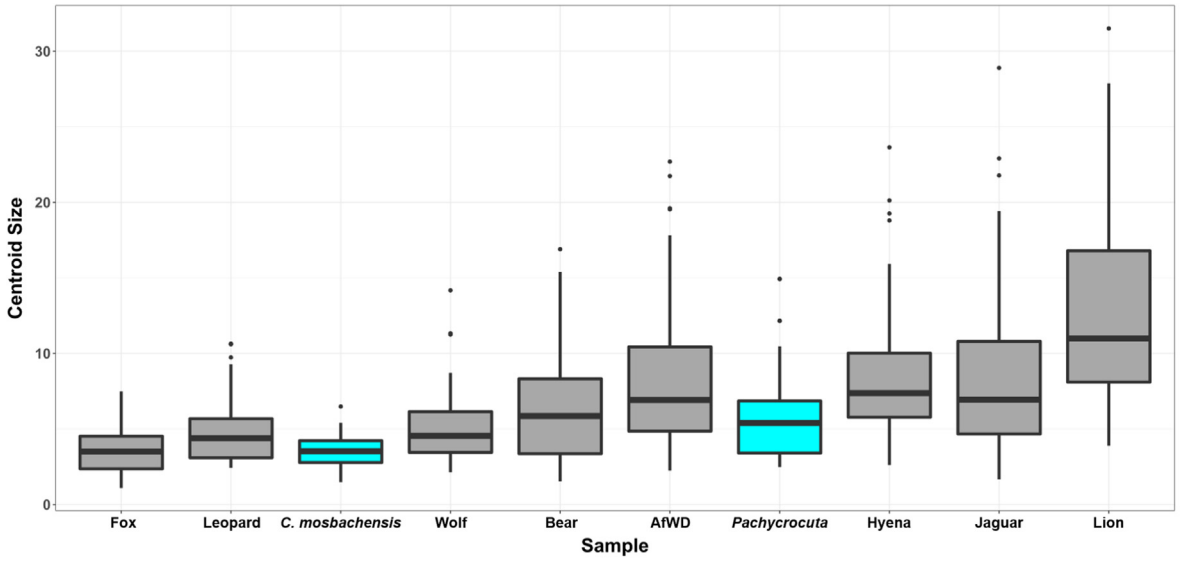

Fig. 7. Graphical representation of the centroid sizes described in Table 4. Highlighted boxplots refer to fossil carnivoran species.

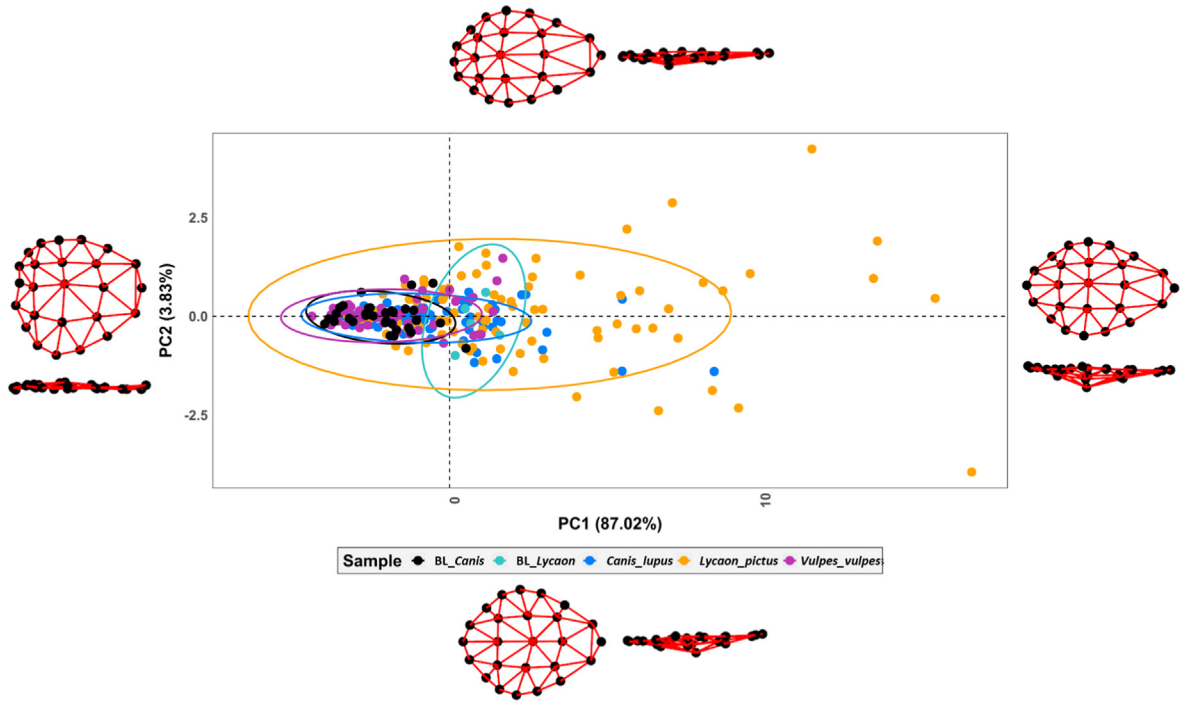

Fig. 8. Principal Component Analysis in form feature space characterizing the tooth pit morphologies of the Barranco León and modern day Canidae samples. Predicted form deformations via thin plate splines are depicted on each extremity of the graph. Form deformations are visualized using a 2.5D Triangulation algorithm.

species, while *Canis mosbachensis* and *Vulpes vulpes* present the least amount of morphological variation dependent on size. CS between both *C. lupus* and *C. mosbachensis* are not the same (TOST $t = -0.8$, $p = 0.98$, $p\ (H_0) = 94.9\%$), with *Canis lupus* producing larger tooth marks than that of *Canis mosbachensis* (Table 4), while CS between *Vulpes vulpes* and *C. mosbachensis* are similar (TOST $t = -3.3$, $p = 0.40$, $p\ (H_0) = 50.1\%$). In this context, *Lycaon pictus* proves to be the member of the Canidae family with the largest and deepest tooth pits, while the five *Lycaon lycaonoides* pits detected in BL-D1 fall well within the 95% confidence interval (TOST $t = -3.8$, $p = 0.86$, $p\ (H_0) = 73.9\%$).

Nevertheless, despite the morphological affinities presented between *Canis lupus* and *Canis mosbachensis*, some multivariate differences in form space can still be noted to some extent (MANOVA $p = 0.009$, FPR = 10.3%). *Lycaon pictus* can be observed to be very different in form space ($p = 0.001$, FPR = 1.8%). This indicates both species of *Canis* to be clearly separable from the *Lycaon* genus, while intra-genus differentiation may be possible.

While the proposed *C. mosbachensis* samples also present morphological affinities with *Vulpes vulpes* as well, the closest early relative of this species, *Vulpes* cf. *alopecoides*, was known to be much smaller than modern day *Vulpes* (Garrido, 2008; Lucenti and

Madurell-Malapeira, 2020). Based on this observation, the original classification results, and the fact that *C. mosbachensis* samples fall between both modern day *C. lupus* and *V. vulpes*, we can confirm our original proposal of assigning these pits to *C. mosbachensis*, defining the morphological variability of these pits to be much closer to *C. lupus*, with a size more similar to modern day *V. vulpes*.

Finally, when computing the difference in calculated meshes obtained from central morphological tendencies, the proposed *C. mosbachensis* sample can be found to present the lowest overall distance with *C. lupus* and *V. vulpes* (Table 5), while appearing very different from *Lycaon pictus*. When observing heat maps that display these differences (Fig. 9), the majority of changes appear across the upper extremities of the pit, likely indicating differences in the circular-like nature described in Fig. 6, as well as around LM5 (the deepest point). It can be seen how *C. mosbachensis* is characterised by more superficial pits, as opposed to the deeper pits produced by *V. vulpes*; a characteristic of which supports the prediction that these pits are closer to *Canis* as opposed to *Vulpes* (Courtenay et al., 2021a). When observing differences with the *Lycaon,* both samples appear to be much deeper than *Canis*, while also presenting stronger deformations in the LM1-LM2 axis of the pit. This indicates a greater elongation in the tooth pit. Finally, when considering *Lycaon pictus* as a reference, it can be observed that the two possible *Lycaon lycaonoides* pits are very similar to *Lycaon pictus* (Table 5), with slight differences in some features of the pit between LM5 and L4.

4.4.2. *Pachycrocuta brevirostris*

The present sample associated to *Pachycrocuta brevirostris* is described by 31 tooth pits in total; 20 tooth pits originally detected from VM3, alongside 11 tooth pits from BL-D1. Similar to the observations made by Yravedra et al. (2022b), the present tooth marks are observed to present greater morphological affinity to modern day *Crocuta crocuta* than any other carnivoran (Table 3). When combining the two samples, these tendencies increase, with those pits associated with *Pachycrocuta brevirostris* appearing slightly closer to *Crocuta crocuta*, while the degree of separation from other samples increases (Table 3). When analysing the differences between samples, VM3 and BL-D1 appear to present strong morphological affinities between each other (Proc. $d = 2.13$, $p = 0.29$). Nevertheless, the tooth marks from BL-D1 appear to be slightly larger (CS mean = 7.3 mm, sd = 1.5, 95% CI = [5.1, 9.3]) than those from VM3 (median = 5.01 mm, MAD = 2.6, 95% CI = [2.5, 12.2]). The combination of these two samples thus captures a broader spectrum of the proposed *Pachycrocuta* tooth mark morphological variability.

As previously observed, allometry is still an important component of Hyaenidae tooth pit morphological variation ($F = 7.6$, $Res.^2 = 0.02$, $ES = 5.80$, $p < 0.001$, FPR <1.8%) (Aramendi et al., 2017; Arriaza et al., 2019, 2021; Courtenay et al., 2021a; Yravedra et al., 2022b), nevertheless, allometric differences between *Crocuta crocuta* and *Pachycrocuta brevirostris* are unimportant ($F = 7.6$, $Res.^2 = 0.016$, $ES = 3.6$, $p = 0.225$, FPR = 47.7%). While the current *Pachycrocuta* pits can be observed to be slightly smaller than *Crocuta crocuta* (Table 4), the magnitude of similarities or differences is not of notable value based on the present data ($t = -2.8$, $p = 0.65$, $p\ (H_0) = 56.7\%$).

Analysis of morphological traits in form space (Fig. 10) reveal both BL-D1 and VM3 samples to greatly overlap with modern day *Crocuta crocuta*. All three Hyaenidae samples can be described by mostly elongated pits, different to those traits previously described for *Canis*, and more similar to the *Lycaon* samples described above. The main morphological patterns that can be described are associated with the position of LM5, and the sliding semilandmarks that shift around it. Similarly, both species of hyaenid present great morphological variance, with the ability to produce a combination of small, large, deep and superficial pits, all within the same sample.

When computing deformations in central configurations (Fig. 9), results only differ slightly from original observations by Yravedra et al. (2022b), in that the change in size is lower than in the present sample, while the average deformation in mesh faces slightly increases from those originally published (0.06 ± 0.04 mm).

5. Discussion

This study presents a detailed analysis and description of tooth pits obtained from level D1 of the Lower Pleistocene site of Barranco León. As has been seen throughout this study, the taphonomic story of BL-D1 is much more complex than originally perceived. In previous research, authors propose *Pachycrocuta brevirostris* as the main carnivoran to have intervened in the formation of BL-D1 (Rodríguez-Gómez et al., 2016; Espigares et al., 2019). Nevertheless, the data obtained here reveal the presence of a larger number of carnivorans, with a notable contribution by a relatively small canid which we have associated with *Canis mosbachensis*, thus shedding new light on the interpretation of this site.

Although the present study has been able to detect the activity of *Pachycrocuta brevirostris*, the impact this carnivoran has had on the formation of BL-D1 site is likely smaller than previously considered (Espigares et al., 2019). First of all, the low overall frequency of tooth marks in BL-D1 is not a likely indicator of hyaenid activity (Espigares et al., 2019; Yravedra et al., 2022b: Supplementary File 6), while only 6 of the tooth pits (9.4%) analysed here have been detected to present morphological affinities with hyaenid species (Table 2). Overall fracture patterns, frequency of furrowing, and a <10 number of tooth marks per specimen (Yravedra et al., 2022a), also contradict patterns produced by hyaenid species (Kuhn et al., 2009).

From a different perspective, the role machairodontine felids had in the Orce sites is frequently proposed as being the primary predator, with hominins and hyaenids opportunistically scavenging the remaining carrion (Palmqvist et al., 2007a,b, 2011; Rodríguez-Gómez et al., 2016). From a taphonomic perspective, however, little evidence has been presented that directly detects the action of these carnivorans in the Orce sites. This is due to the proposal that machairodontine felids are unlikely to mark bone during feeding (Marean, 1989; Palmqvist et al., 2007a,b). While this hypothesis is supported by compelling biomechanical data (Palmqvist et al.,

Table 5
Description of distances (mm) from the reference mesh to the compared mesh, visualized graphically in Fig. 9.

	Lycaon pictus				Canis lupus				Vulpes vulpes			
	Min	Central	Dev.	Max	Min	Central	Dev.	Max	Min	Central	Dev.	Max
L. pictus	0.00	0.00	0.00	0.00	0.06	0.34	0.20	0.64	0.09	0.53	0.27	0.98
L. lycaonoides	0.00	0.04	0.04	0.17	0.04	0.33	0.19	0.56	0.11	0.52	0.25	0.88
C. lupus	0.03	0.07	0.02	0.13	0.00	0.00	0.00	0.00	0.00	0.16	0.11	0.34
C. mosbachensis	0.09	0.11	0.02	0.15	0.00	0.03	0.02	0.06	0.00	0.01	0.01	0.03
V. vulpes	0.08	0.10	0.02	0.14	0.00	0.02	0.02	0.05	0.00	0.00	0.00	0.00

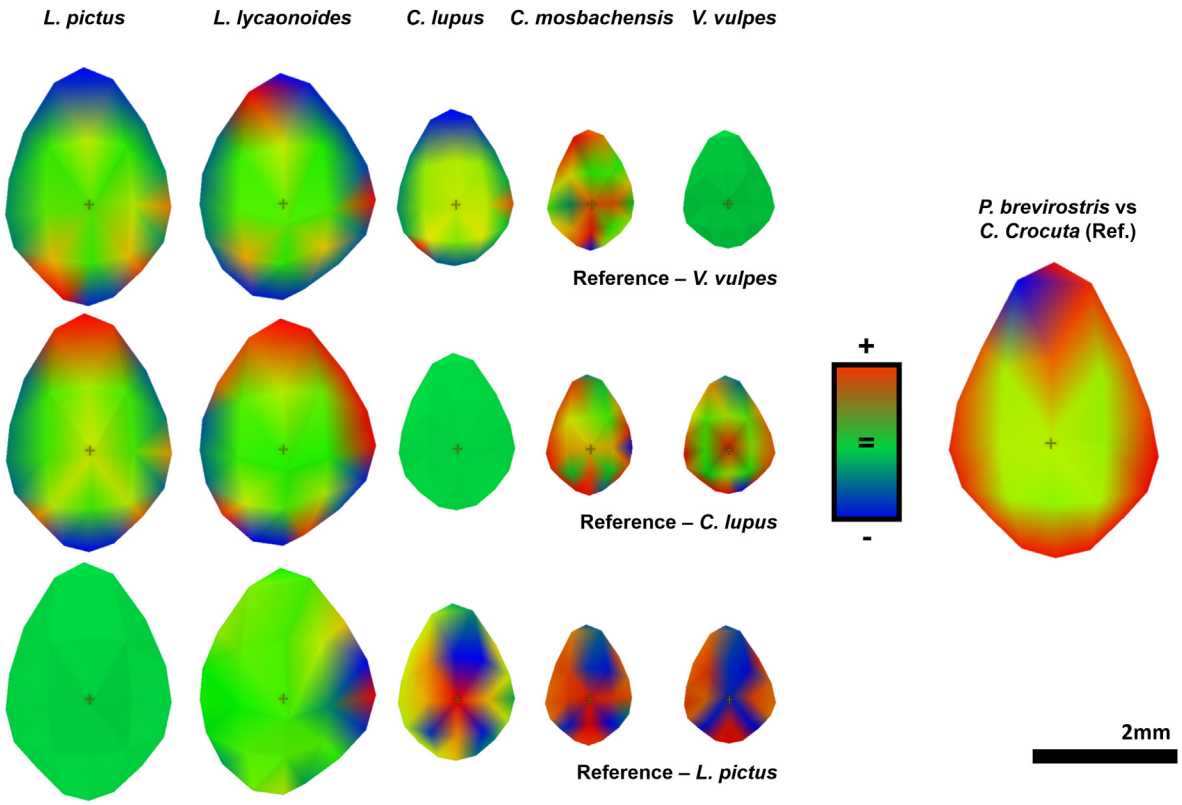

Fig. 9. Heatmaps obtained from 3D meshes, computed using the central configuration of each carnivoran sample. Changes in colour indicate how similar one mesh is when compared with the reference mesh, with shades of blue indicating negative deformations and shades of red indicating positive deformations. (For interpretation of the references to colour in this figure legend, the reader is referred to the Web version of this article.)

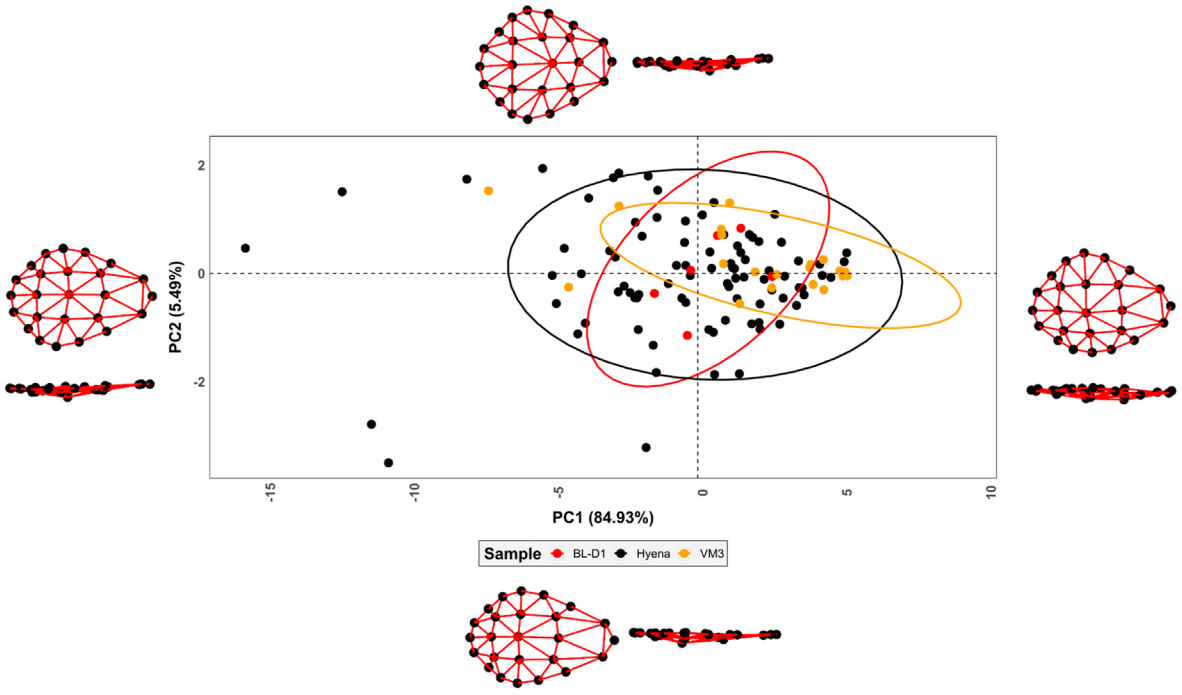

Fig. 10. Principal Component Analysis in form feature space characterizing the tooth pit morphologies of the Barranco León, Venta Micena 3, and modern day Hyaenidae samples. Predicted form deformations via thin plate splines are depicted on each extremity of the graph. Form deformations are visualized using a 2.5D Triangulation algorithm.

2007a,b), it is important to note that tooth marks are often accidental. Furthermore, data from other sites have still been able to attribute the presence of tooth marks to machairodontine feeding habits (Marean and Ehrhardt, 1995; Domínguez-Rodrigo et al.,

2022). In light of this, bite damage cannot be exclusively related to the chewing or consumption of bone-related nutrients, highlighting a lack of evidence to say that machairodontines were not able to produce tooth marks, just less likely.

While both *Pachycrocuta* and *Homotherium* have been identified here as being likely contributors to both the BL-D1 and VM3 assemblages (Yravedra et al., 2022b), the majority of data from the present sample has been found to be product of *Canis mosbachensis* activity ($n = 33$; 51.6%). *Canis mosbachensis* is mostly known as an omnivorous species (Palmqvist et al., 2008), of smaller size than modern day *Canis lupus*. Modern day *Canis lupus* are social hunters, enabling them to hunt prey larger than themselves (Gittleman, 1985; Vezina, 1985; Yravedra et al., 2011). Nevertheless, considering the physiology of *Canis mosbachensis*, as well as the significantly larger trophic pressure observed in the Early Pleistocene carnivoran guild of Guadix Baza (Rodríguez et al., 2012; Lozano et al., 2016), it is unlikely that *Canis mosbachensis* would have been the predator responsible for the large ungulate carcasses recovered from BL-D1. From this perspective, and also considering the adult-rich age profiles (Yravedra et al., 2022a), *Canis mosbachensis* can be interpreted to have had a secondary role in the modification of fossils. This is especially relevant when considering tooth marks made by different carnivorans on the same specimen (Table 2), implying *Canis mosbachensis* to have scavenged the kills of other carnivorans, such as *Homotherium latidens*.

From the perspective of the other taphonomic agents, remains of both *Lycaon lycaonoides* and *Ursus etruscus* have been identified in BL-D1, represented by a single adult individual each (Espigares et al., 2019; Yravedra et al., 2022a). Here we have been even able to infer the interaction of these species with the assemblage, as seen through the presence of 5 and 7 tooth marks respectively. While *Ursus etruscus* is believed to be an omnivorous species, primarily feeding on plants (Palmqvist et al., 2008; Medin et al., 2017), most bears, such as the brown bear (*Ursus arctos*), are known to scavenge and sporadically hunt (Mattson, 1997). Likewise, ursids from the Venta Micena localities have also been interpreted to present an increased intake of animal based foods (Medin et al., 2017). *Lycaon,* on the other hand, are hypercarnivorous hunters (Estes and Goddard, 1967; Malcolm and Van-Lawick, 1975; Rhodes and Rhodes, 2004). Nevertheless, modern-day African Wild Dogs are not known for generating intense bone surface modifications (Yravedra et al., 2013; Fourvel et al., 2018). In light of these observations, the importance of the present study can be found in the ability to detect these carnivorans, despite their lack of general prevalence as taphonomic agents in many sites. Likewise, while the present study has been unable to specify the precise agents responsible for the smaller marks in BL-D1, the presence of smaller carnivorans such as mustelids in the Guadix Baza region (Madurell-Malapeira et al., 2011; Martínez-Navarro et al., 2010; Ros-Montoya et al., 2021), suggest that they could be a plausible candidate for these marks. Nevertheless, the possibility that other larger carnivorans, external to and not yet detected in this region, could have entered the site and left marks. Finally, the presence of anthropogenic modifications in BL-D1 cannot be ignored (Yravedra et al., 2022a), especially considering the 9 specimens observed to have both cut and tooth marks. While, in general, the percentages of cut and percussion marked bones are relatively low, their location across the appendicular skeleton indicate early access of hominins to the animal resources at this site. Among these evidence, authors have identified both filleting and evisceration activities by human populations (Espigares et al., 2019; Yravedra et al., 2022a). Nevertheless, a more detailed investigation must be carried out into the nature of these alterations.

Finding direct analogies with fossil carnivorans is a complicated process, conditioned by the fragile and incomplete nature of the fossil record. While it is impossible to state with 100% confidence the precise agents intervening in a site (Marean and Ehrhardt, 1995), the proposed methodological approaches can be considered a more empirical advance in identifying these agents (Courtenay et al., 2019, 2021a; Courtenay and González-Aguilera, 2020). The use of computational learning algorithms has been able to make predictions with 88.77 ± 7.49% confidence, assigning each tooth pit to their closest modern day analogy. In light of these calculations, as well as the assessment of Procrustes distances and centroid sizes, this can be considered a valuable new perspective on the interpretation of archaeological and palaeontological sites.

The original hypotheses surrounding the interpretation of the Orce sites primarily identifies *Pachycrocuta* and hominins as the sole modifiers of bones. From the perspective of carnivorans, this theory is based on the “large size” of tooth pits (Espigares et al., 2019). The assumption that large tooth pits are indicatory of *Pachycrocuta* excludes the fact that tooth pits are often produced accidently. Therefore, while large felids may not have been consumers of bone-type nutrients, this does not imply that machairodontines could not have left tooth pits. Likewise, modern day lions are not osteo or durophagic, yet still leave tooth marks (Gidna et al., 2013). Here we have shown that the larger tooth pits of BL-D1 present a greater morphological affinity to Felidae (Proc. $D = 1.125$), than Hyaenidae (4.054). While it could be argued that allometry is conditioning these results, if size is eliminated from analyses, Procrustes distances of shape still reveal these tooth marks to be analogous with a species of felid, over *Crocuta crocuta* (Table 6). Moreover, over 50% of the present sample have been associated with *Canis mosbachensis*, which are closer in morphology to smaller canids than *Pachycrocuta* (Table 6). While Procrustes distances in form space approximate these marks to *Vulpes* as well, shape space highlights the affinities with *Canis* (Table 6), thus enforcing our predictions. Finally, as seen in the present sample, the majority of tooth pits analysed would fall into the range of smaller carnivorans (Andrés et al., 2012, Fig. 5), which contradicts the *Pachycrocuta* based hypothesis.

From the perspective of inter-carnivoran competition for resources, the observation that multiple carnivorans fed on the same bone could be of great interest to taphonomic research. While a possibility remains that some of these examples of “competition” are misclassifications by the algorithms, the morphological

Table 6
– Procrustes distances of shape between each of the fossil carnivore species detected, and their modern day analogues. Both the Pachycrocuta and Homotherium samples include tooth pits detected from Barranco León and Venta Micena 3 (Yravedra et al. 2022b).

	C. lupus	L. pictus	C. crocuta	U. arctos	*P. leo*	P. onca	P. pardus	V. vulpes
C. mosbachensis	0.043	0.060	0.060	0.087	0.069	0.078	0.082	0.050
L. lycaonoides	0.082	0.092	0.101	0.109	0.100	0.112	0.120	0.116
*P. brevirostris**	0.036	0.039	0.032	0.053	0.051	0.048	0.046	0.042
*P. brevirostris***	0.035	0.041	0.032	0.053	0.054	0.050	0.048	0.043
U. etruscus	0.062	0.075	0.086	0.062	0.090	0.079	0.079	0.112
H. latidens	0.062	0.051	0.054	0.059	0.062	0.046	0.046	0.067

affinities described by Procrustes distances, and differences in tooth mark sizes, seem to support a differential classification. Future research into the spatial distribution of these traces may help develop our understanding of the order in which different species intervened on carrion (Parkinson et al., 2014, 2015, 2022; Parkinson, 2018; Mora et al., 2022).

In summary, the trophic pressure of the Orce region is of increasing complexity, with evidence of multiple agents competing for resources in the same region. While the most logical hypothesis would place large felids at the top of the food chain, it cannot be denied that both *Pachycrocuta* (Kruuk, 1972; Bearder, 1977; Tilson and Henschel, 1986; Mills, 1984a & b; Henshel, 1986; Cooper, 1990; Turner and Antón, 1996) and hominins (Domínguez-Rodrigo, 1999; Domínguez-Rodrigo et al., 2007), could have played a major role in this ecosystem. From this perspective, BL-D1 can be considered a palimpsest where both carnivorans and hominins would have had to frequently adapt to survive.

6. Conclusion

In this paper, 3D modelling, geometric morphometrics, and computational learning were used to provide new insights into the tooth pits observed on faunal materials at Barranco León (Orce, Granada, Spain). Regardless of the scenario, here we present empirical data that strongly implicate the morphological affinities between the tooth marks of BL-D1 with the genus *Canis*. While errors may exist, the present study has based the identification of fossil carnivoran species on an extensive collection of modern analogues. Likewise, this study has been able to detect a number of different carnivorans, including; canids, large felids, hyaenids and ursids, sometimes interacting on the same bones. The most notable carnivore to have been estimated to have intervened in BL-D1 being *Canis* mosbachensis. These observations thus add to the ecological complexity of the Guadix Baza region and highlight a more prominent role of large canids in the southern European Early Pleistocene.

From this perspective, the data collected can be considered a valuable and novel reference collection for the study of extinct carnivoran species. Nevertheless, the site of Barranco León is still under excavation, and a larger sample could be considered fundamental so as to provide an in depth characterization and interpretation of the site.

The nature of the BL-D1 palimpsest is thus gradually appearing to be much more complex than originally perceived, shedding new light on the hominin populations ≈1.4 Ma in the Guadix-Baza region. As can be seen, a number of carnivores contributed to this accumulation, mixing the fossil remains with those that may have already been present. From this perspective, computational learning and robust statistics can be considered a valuable contribution to deciphering hominin activities in the taphonomic register.

Funding

This research was funded by the Junta de Andalucía, Consejería de Cultura: Orce Research Project "Primeras ocupaciones humanas y contexto plaeoecológico a partir de los depósitos pliopleitocenos de la cuenca de Guadix-Baza: zona arqueológica de la Cuenca de Orce (Granada, España), 2017–2020" (Ref: BC.03.032/17). We also received support from the PALARQ Foundation with the convocatory of Analitics 2019): "Identificando Carnívoros a partir de análisis Tafonómicos de última generación aplicando Fotogrametría y Morfometría Geométrica de las Marcas de Diente. Aplicación a Yacimientos del Pleistoceno Inferior Ibérico: FN3, Venta Micena 3y 4 (Granada), Pontón de la Oliva (Patones, Madrid)". This work is also funded by the Spanish Ministry of Science and Innovation with the call for funding "Proyectos Generación de Conocimiento 2021: Challenges and research opportunities in the Pleistocene Archaeological Sites of the Guadix-Baza Basin (Granada, Spain). Cuenca de Orce and Solano del Zamborino (ORCEpluSZ)" (Ref: PID2021-125098NB-I00).

L.A.C. is funded by the Spanish Ministry of Science, Innovation and Universities, with an FPI Predoctoral Grant (Ref. PRE2019-089411), associated to project RTI2018-099850-B-I00 and the University of Salamanca. D.H.R. was supported by the Ministry of Science, Innovation and Universities, under the contract REF: PEJ2019-005420-A as part of the i + D + I Garantía Juvenil.

Author contributions

Lloyd A. Courtenay – Conceptualization, methodology, software, validation, formal analysis, investigation, data curation, writing – original draft, review and editing, visualization. **José Yravedra** – Formal analysis, investigation, data curation, resources, writing – original draft, review and editing, supervision, project administration, funding acquisition. **Darío Herranz-Rodrigo** – Data curation. **Juan José Rodríguez-Alba** – Writing – reviewing and editing. **Alexia Serrano-Ramos** – Data curation. **Verónica Estaca-Gómez** – Writing – reviewing and editing. **Diego González-Aguilera** – Resources, writing – reviewing and editing, supervision, funding acquisition. **José Antonio Solano** – Data curation, supervision. **Juan Manuel Jiménez-Arenas** – Resources, supervision, Project administration, funding acquisition.

Declaration of competing interest

The authors declare that they have no known competing financial interests or personal relationships that could have appeared to influence the work reported in this paper.

Data availability

Data has been provided as supplementary materials

Aknowledgements

We would like to thank all researchers, students and volunteers involved in the excavations, preparations and study of Barranco Léon. The corresponding author would also like to thank Rosa Huguet for her helpful comments and suggestions. Finally, the corresponding author is very grateful for the comments and suggestions made by Julia Aramendi to improve the quality of this line of research. We would also like to thank Jean-Philip Brugal, Antoine Souron, and one anonymous, reviewer for their constructive comments on earlier versions of this manuscript.

Appendix A. Supplementary data

Supplementary data to this article can be found online at https://doi.org/10.1016/j.quascirev.2022.107912.

References

Alcántara-García, V., Barba Egido, R., Barral del Pino, J.M., Crespo Ruiz, A.B., Eiriz Vidal, A.I., Falquina Aparicio, Á., Herrero Calleja, S., Ibarra Jiménez, A., Megías González, M., Pérez Gil, M., Pérez Tello, V., Rolland Calvo, J., Yravedra, J., Vidal, A., Domíngez-Rodrigo, M., 2006. Determinación de procesos de fractura sobre huesos: un sistema de análisis de los ángulos de los planos de fracturación como discriminador de agentes bióticos. Trab. Prehist. 61 (1), 25–38.

Anadón, P., Gabás, M., 2009. Paleoenvironmental evolution of the early Pleistocene lacustrine sequence at Barranco León archeological site (Orce, Baza basin,

southern Spain) from stable isotopes and Sr and Mg chemistry of ostracod shells. J. Paleolimnol. 42, 261–279. https://doi.org/10.1007/s10933-008-9275-6.
Anadón, P., Juliá, R., Oms, O., 2003. Estratigrafía y estudio sedimentológico preliminar de diversos afloramientos en Barranco León y Fuente Nueva (Orce, Granada). In: Toro, I., Agustí, J., Martínez, B. (Eds.), El Pleistoceno inferior de Barranco León y Fuente Nueva 3, Orce (Granada). Memoria científica Campañas 1999-2002, Monografías de Arqueología, vol. 17. Junta de Andalucía. Consejería de Cultura, pp. 47–72.
Anadón, P., Oms, O., Violeta, R., Ramon, J., 2015. The geochemistry of biogenic carbonates as a paleoenvironmental tool for the Lower Pleistocene Barranco León sequence (BL-5D, Baza Basin, Spain). Quat. Int. 389, 70–83.
Andrés, M., Gidna, A.O., Yravedra, J., Domínguez-Rodrigo, M., 2012. A study of dimensional differences of tooth marks (pits and scores) on bones modified by small and large carnivores. Archaeological and Anthropological Sciences 4 (3), 209–219. https://doi.org/10.1007/s12520-012-0093-4.
Antón, M., 2013. Sabertooth. Indiana University Press.
Antón, M., Galobart, A., Turner, A., 2005. Co-existence of scimitar-toothed cats, lions and hominins in the European Pleistocene. Implications of the post-cranial anatomy of *Homotherium latidens* (Owen) for comparative palaeoecology. Quat. Sci. Rev. 24 (10–11), 1287–1301. https://doi.org/10.1016/j.quascirev.2004.09.008.
Antón, M., Salesa, M.J., Galobart, A., Tseng, Z.J., 2014. The Plio-Pleistocene scimitar-toothed felid genus *Homotherium* Fabrini, 1890 (Machairodontinae, Homotherini): diversity, palaeogeography and taxonomic implications. Quat. Sci. Rev. 96, 259–268. https://doi.org/10.1016/j.quascirev.2013.11.022.
Aramendi, J., Maté-González, M.A., Yravedra, J., Ortega, M.C., Arriaza, M.C., González-Aguilera, D., Baquedano, E., Domínguez-Rodrigo, M., 2017. Discerning carnivore agency through the three-dimensional study of tooth pits: revisiting crocodile feeding behaviour at FLK- Zinj and FLK NN3 (Olduvai Gorge, Tanzania). Palaeogeogr. Palaeoclimatol. Palaeoecol. 488, 93–102. https://doi.org/10.1016/j.palaeo.2017.05.021.
Arriaza, M.C., Aramendi, J., Maté-González, M.A., , Yravedra, J. D., Strantdford, D., 2019. Characterising leopard as taphonomic agent throught the use of Micro-photogrammetric reconstruction of tooth marks and pit to score ratio. Hist. Biol. https://doi.org/10.1080/08912963.2019.1598401.
Arriaza, M.C., Aramendi, J., Maté-González, M.A., Yravedra, J., Stratford, D., 2021. The hunted or the scavenged? Australopith accumulation by brown hyenas at Sterkfontein (South Africa). Quat. Sci. Rev. 273, 107252. https://doi.org/10.1016/j.quascirev.2021.107252.
Barsky, D., Celiberti, V., Cauche, D., Grégoire, S., Lebègue, F., Lumley, H., Toro Moyano, I., 2010. Raw material discernment and technological aspects of the Barranco León and Fuente Nueva 3 stone assemblages (Orce southern Spain). Quat. Int. 223–224, 201–219. https://doi.org/10.1016/j.quaint.2009.12.004.
Barsky, D., Vergès, J.M., Sala, R., Menendez, L., Toro-Moyano, I., 2015a. Limestone percussion tolos from the late early Pleistocene sites of Barranco León and Fuente Nueva 3 (Orce, Spain). Philos. Trans. R. Soc. Lond. B Biol. Sci. 370, 1682. https://doi.org/10.1098/rstb.2014.0352.
Barsky, D., Sala, R., Menéndez, L., Toro-Moyano, I., 2015b. Use and re-use: Re-knapped flakes from the mode 1 site of Fuente Nueva 3 (Orce, Andalucía, Spain). Quat. Int. 361, 21–33. https://doi.org/10.1016/j.quaint.2014.01.048.
Bearder, S.K., 1977. Feeding habits of spotted hyaenas in a woodland habitat. East Afr. Wildl. J. 15, 263–280.
Benjamin, D.J., Berger, J.O., 2019. Three recommendations for improving the use of p-values. Am. stat. 73, 186–191.
Binford, L.R., 1981. Bones: Ancient Men and Modern Myths. Academic Press, Inc., New York.
Blain, H.A., Bailon, S., Agustí, J., Martínez-Navarro, B., Isidro, T., 2011. Paleoenvironmental and paleoclimatic proxies to the Early Pleistocene hominids of Barranco León D and Fuente Nueva 3 (Granada, Spain) by means of their amphibian and reptile assemblages. Quat. Int. 243 (1), 44–53.
Blain, H.A., Lozano-Fernández, I, Agustí, J., Bailon, S., Menéndez Granda, L., Espígares Ortiz, Ros-Montoya, S., Jiménez Arenas, J.M., Toro-Moyano, I., Martínez-Navarro, B., Sala, R., 2016. Refining upon the climatic background of the Early Pleistocene hominid settlement in western Europe: Barranco León and Fuente Nueva-3 (Guadiz-Baza Basin, SE Spain). Quat. Sci. Rev. 144, 132–144.
Blumenschine, R.J., 1995. Percussion marks, tooth marks, and experimental determinations of the timing of hominid and carnivore access to long bones at FLK Zinjanthropus, Olduvai Gorge, Tanzania. J. Hum. Evol. 29, 21e51.
Blumenschine, R.J., Marean, C.W., Capaldo, S.D., 1996. Blind tests of interanalyst correspondence and accuracy in the identification of cut marks, percussion marks, and carnivore tooth marks on bone surfaces. J. Archeol. Sci. 23, 493e507.
Bookstein, F.L., 1989. Principal warps: thin-Plate Splines and the decomposition of deformations. IEEE Trans. Pattern Anal. Mach. Intell. 11 (6), 567–585.
Bookstein, F.L., 1991. Morphometric Tools for Landmark Data. Cambridge University Press, Cambridge.
Bookstein, F.L., 1997. Landmark methods for forms without landmarks: morphometrics of group differences in outline shape. Med. Image Anal. 1, 225–243.
Bourguignon, L., Crochet, J.-Y., Capdevila, R., Ivorra, J., Antoine, P.-O., Agustí, J., Barsky, D., Blain, H.-A., Boubles, N., Bruxelles, L., Claude, J., Cochard, D., Filoux, A., Firmat, C., Lozano-Fernández, I., Magniez, P., Pelletier, M., Rios-Garaizar, J., Testu, A., Valensi, P., De Weyer, L., 2016. Bois-de-Riquet (Lézignan-la-Cèbe, Hérault): a late Early Pleistocene archeological occurrence in southern France. Quat. Int. 393, 24–40. https://doi.org/10.1016/j.quaint.2015.06.037.
Brain, C.K., 1981. Hunters or the Hunted? an Introduction to African Cave Taphonomy. University of Chicago Press, Chicago.
Bunn, H.T., 1982. Meat Eating and Human Evolution: Studies on the Diet and Subsistence Patterns of Plio-Pleistocene Hominids in East Africa. PhD Thesis. University of California, Berkeley.
Bunn, H.T., Pickering, T.R., 2010. Methodological recommendations for ungulate mortality analyses in paleoanthropology. Quat. Res. 74, 388–394.
Cheheb, R.C., Arzarello, M., Arnaud, J., Berto, C., Cáceres, I., Caracausi, S., Colopi, F., Daffara, S., Canini, G.M., Huguet, R., Karambatsou, T., Benedetto, S., Zambaldi, M., Berruti, G.L.F., 2019. Human behaviour and Homo-mammal interactions at the first European peopling: new evidence from the Pirro Nord site (Apricena, Southern Italy). Sci. Nat. 106, 16. https://doi.org/10.1007/s00114-019-1610-4.
Colquhoun, D., 2019. The False Positive Risk: a proposal concerning what to do about p-values. Am. Statistician 73, 192–201.
Cooper, S.M., 1990. The hunting behaviour of spotted hyaenas (*Crocuta crocuta*) in a region containing both sedentary and migratory populations of herbivores. Afr. J. Ecol. 28 (2), 131–141. https://doi.org/10.1111/j.1365-2028.1990.tb01145.x.
Courtenay, L.A., González-Aguilera, D., 2020. Geometric morphometric data augmentation using generative computational learning algorithms. Appl. Sci. 10 (24), 9133. https://doi.org/10.3390/app10249133.
Courtenay, L.A., Yravedra, J., Huguet, R., Aramendi, J., Maté-González, M.Á., González-Aguilera, D., Arriaza, M.C., 2019. Combining machine learning algorithms and geometric morphometrics: a study of carnivore tooth marks. Palaeogeogr. Palaeoclimatol. Palaeoecol. 522, 28–39. https://doi.org/10.1016/j.palaeo.2019.03.007.
Courtenay, L.A., Yravedra, J., Maté-González, M.Á., Vázquez-Rodríguez, J.M., Fernández-Fernández, M., González-Aguilera, D., 2020a. The effects of prey size on carnivore tooth mark morphologies on bone; the case study of *Canis lupus signatus*. Hist. Biol. 33 (11), 2760–2772. https://doi.org/10.1080/08912963.2020.1827239.
Courtenay, L.A., Herranz-Rodrigo, D., Huguet, R., Maté-González, M.Á., González-Aguilera, D., Yravedra, J., 2020b. Obtaining new resolutions in carnivore tooth pit morphological analyses: a methodological update for digital taphonomy. PLoS One 15 (10), e0240328. https://doi.org/10.1371/journal.pone.0240328.
Courtenay, L.A., Herranz-Rodrigo, D., González-Aguilera, D., Yravedra, J., 2021a. Developments in data science solutions for carnivore tooth pit classification. Sci. Rep. 11, 10209. https://doi.org/10.1038/s41598-021-89518-4.
Courtenay, L.A., Herranz-Rodrigo, D., Yravedra, J., Vázquez-Rodríguez, J., Huguet, R., Barja, I., Maté-González, M.A., Fernández, M., González-Aguilera, D., 2021b. Effects of captivity on carnivore implications in ecological studies of both the past and present. Animals 11, 2323. https://doi.org/10.3390/ani11082323.
Courtenay, L.A., González-Aguilera, D., Lagüela, S., del Pozo, S., Ruiz-Mendez, C., Barbero-García, I., Román-Curto, C., Cañueto, J., Santos-Durán, C., Cardeñoso-Álvarez, M.E., Roncero-Riesco, M., Hernandez-López, D., Guerrero-Sevilla, D., Rodríguez-Gonzalvez, P., 2021c. Hyperspectral imaging and robust statistics in non-melanoma skin cancer analysis. Biomed. Opt Express 12 (8), 5107–5127.
Domínguez-Rodrigo, M., 1997. Meat-eating by early Hominids at the FLK 22 Zinjanthropus Site, Olduvai Gorge, Tanzania: an experimental approach using cut mark data. J. Hum Evol. 33 (6), 669–690.
Domínguez-Rodrigo, M., 1999. Flesh availability and bone modifications in carcasses consumed by lions, palaeoecological relevance in hominind foraging patterns. Palaeogeogr. Palaeoclimatol. Palaeoecol. 149, 373–388.
Domínguez-Rodrigo, M., Barba, R., 2006. New estimates of tooth mark and percussion mark frequencies at the FLK Zinj site: the carnivore-hominid-carnivore hypothesis falsified. J. Hum. Evol. 50 (2), 170–194.
Domínguez-Rodrigo, M., Barba, R., Egeland, C., 2007. Deconstructing Olduvai. Springer, The Netherlands.
Domínguez-Rodrigo, M., Gidna, A.O., Yravedra, J., Musiba, C., 2012. A comparative neo-taphonomic study of felids, hyaenids and canids: an analogical framework based on long bone modification patterns. J. Taphon. 10 (3), 147–164.
Domínguez-Rodrigo, M., Yravedra, J., Organista, E., Gidna, A., Fourvel, J.-B., Baquedano, E., 2015. A new methodological approach to the taphonomic study of paleontological and archaeological faunal assemblages: a preliminary case study from Olduvai Gorge (Tanzania). J. Archaeol. Sci. 59, 35–53. https://doi.org/10.1016/j.jas.2015.04.007.
Domínguez-Rodrigo, M., Egeland, C.P., Cobo-Sánchez, L., Baquedano, E., Hulbert, R.C., 2022. Sabertooth carcass consumption behavior and the dynamics of Pleistocene large carnivoran guilds. Sci. Rep. 12 (1), 6045. https://doi.org/10.1038/s41598-022-09480-7.
Echassoux, A., 2004. Étude taphonomique, paléoécologique et archéozoologique des faunes de grands mammifères de la seconde moitié du Pléistocène inférieur de la grotte du Vallonet (Roquebrune-Cap-Martin, Alpes-Maritimes, France). L'anthropologie. 108, 11–53.
Espigares, M.P., Martínez-Navarro, B., Palmqvist, P., Ros-Montoya, S., Toro, I., Agustí, J., Sala, R., 2013. *Homo* vs. *Pachycrocuta*: earliest evidence of competition for an elephant carcass between scavengers at Fuente Nueva-3 (Orce, Spain). Quat. Int. 295, 113–125. https://doi.org/10.1016/j.quaint.2012.09.032.
Espigares, M.P., Palmqvist, P., Guerra-Merchán, A., Ros-Montoya, S., García-Aguilar, J.M., Rodríguez-Gómez, G., Serrano, F.J., Martínez-Navarro, B., 2019. The earliest cut marks of Europe: a discussion on hominin subsistence patterns in the Orce sites (Baza basin, SE Spain). Sci. Rep. 9, 15408. https://doi.org/10.1038/s41598-019-51957-5.
Estes, R.D., Goddard, J., 1967. Prey selection and hunting behaviour of the african wild dog. J. Wildl. Manag. 31, 52–69. https://doi.org/10.2307/3798360.
Fourvel, J.P., Magniez, P., Moigne, A.M., Testu, A., Joris, A., Lamglait, B., Vaccaro, C., Fosse, P., 2018. Wild dogs and their relatives: implication of experimental feedings in their taphonomical identification. Quaternaire 29 (1), 21–29.

https://doi.org/10.4000/quaternaire.8578.
Garrido, G., 2008. El registro de *Vulpes alopecoides* (Forsyth-Major, 1877), *Canis etruscus* (Forsyth-Major, 1877) y *Canis* cf. *Falconeri* (Forsyh-Major, 1877) (Canidae, carnívora, mammalia) en Fonelas P-1 (Cuenca de Guadix, Granada). In: Arribas, A. (Ed.), Vertebrados del Plioceno superior terminal en el suroeste de Europa: Fonelas P-1 y el Proyecto Fanals. Cuadernos del Museo Geominero, nº10. Instituto Geológico y Minero de España, Madrid.
Gibert, J., Gibert, L., Iglesias, A., Maestro, E., 1998. Two 'Oldowan' assemblages in the Plio-Pleistocene deposits of the Orce region, southeast Spain. Antiquity 72, 17–25. https://doi.org/10.1017/S0003598X00086233.
Gidna, A.J., Yravedra, J., Domínguez-Rodrigo, M., 2013. A cautionary note on the use of captive carnivores to model wild predator behaviour: a comparison of bone modification patterns on long bones by captive and wild lions. J. Archaeol. Sci. 40, 1903–1910.
Gittleman, J.L., 1985. Carnivore body size: ecological and taxonomic correlates. Oecologia (Berl.) 67 (4), 540–554. https://doi.org/10.1007/BF00790026.
Goodfellow, I., Bengio, Y., Courville, A., 2016. Deep Learning. MIT Press, Cambridge.
Gunz, P., Mitteroecker, P., 2013. Semilandmarks: a method for quantifying curves and surfaces. Hystrix it. J. Mammal. 24, 103–109. https://doi.org/10.4404/hystrix-24.1-6292.
Haynes, G., 1980. Evidence of carnivore gnawing on Pleistocene and recent mammalian bones. Paleobiology 6 (3), 341–351.
Haynes, G., 1983. A guide for differentiating mammalian carnivore taxa responsible for gnaw damage to herbivore limb bones. Paleobiology 9 (2), 164–172.
Henshel, J.R., 1986. The Socio-Ecology of Spotted hyaena *Crocuta crocuta* in the Kruger National Park. Ph.D. thesis, University of Pretoria.
Höhle, J., Höhle, M., 2009. Accuracy assessment of digital elevation models by means of robust statistical methods. ISPRS J. Photogrammetry Remote Sens. 64, 398–406. https://doi.org/10.1016/j.isprsjprs.2009.02.003.
Huguet, R., Saladié, P., Cáceres, I., Díez, C., Rosell, J., Bennàsar, M., Blasco, R., Esteban-Nadal, M., Gabucio, M.J., Rodríguez-Hidalgo, A., Carbonell, E., 2013. Successful subsistence strategies of the first humans in south-western Europe. Quat. Int. 295, 168–182.
Kruuk, H., 1972. The Spotted Hyena: A Study of Predation and Social Behavior. University of Chicago Press, Chicago.
Kuhn, B.F., Berger, L.R., Skinner, J.D., 2009. Variation in tooth mark frequencies on long bones from the assemblages of all three extant bone-collecting hyaenids. J. Archaeol. Sci. 36 (2), 297–307. https://doi.org/10.1016/j.jas.2008.09.008.
Lakens, D., 2017. Equivalence tests: a pratical primer for T tests, correlations and meta analyses. Society of Psychological and Personality Sciences 8 (4), 355–362. https://doi.org/10.1177/1948550617697177.
Lopez-Fernandez, L., Rodriguez-Gonzalvez, P., Hernandez-Lopez, D., Ortega-Terol, D., González-Aguilera, D., 2017. Comparative analysis of triangulation libraries for modeling large point clouds from land and their infrastructures. Infrastructure 2 (1), 1–11. https://doi.org/10.3390/infrastructures2010001.
Lozano, S., Mateos, A., Rodríguez, J., 2016. Exploring paleo food-webs in the European Early and Middle Pleistocene: a network analysis. Quat. Int. 413, 44–54. https://doi.org/10.1016/j.quaint.2015.10.068.
Lucenti, S.B., Madurell-Malapeira, J., 2020. Unraveling the fossil record of foxes: an updated review on the Plio-Pleisotcene *Vulpes* spp. from Europe. Quat. Int. 236, 106296. https://doi.org/10.1016/j.quascirev.2020.106296.
Luzón, C., Yravedra, J., Courtenay, L.A., Saarinen, J., Blain, H.-A., DeMiguel, D., Viranta, S., Azanza, B., Rodríguez-Alba, J.J., Herranz-Rodrigo, D., Serrano-Ramos, A., Solano, J.A., Oms, O., Agustí, J., Fortelius, M., Jiménez-Arenas, J.M., 2021. Taphonomic and spatial analyses from the early Pleistocene site of Venta Micena 4 (Orce, Guadix-Baza Basin, southern Spain). Sci. Rep. 11 (1). https://doi.org/10.1038/s41598-021-93261-1.
Madurell-Malapeira, J., Martínez-Navarro, B., Ros-Montoya, S., Patrocinio Espigares, M., Toro, I., Palmqvist, P., 2011. The earliest European badger (*Meles meles*), from the late villafranchian site of Fuente Nueva 3 (Orce, Granada, SE iberian peninsula). Comptes Rendus Palevol 10 (8), 609–615. https://doi.org/10.1016/j.crpv.2011.06.001.
Malcolm, J.R., Van Lawick, B., 1975. Notes on wild dogs (*Lycaon pictus*) hunting zebras. Mammalia 39, 231–240. https://doi.org/10.1515/mamm.1975.39.2.231.
Marean, C.W., 1989. Sabertooth cats and their relevance for early hominid diet and evolution. J. Hum. Evol. 18, 559–582. https://doi.org/10.1016/0047-2484(89)90018-3.
Marean, C.W., Ehrhardt, C.L., 1995. Palaeanthropological and palaeoecological implications of the taphonomy of a sabertooth's den. J. Hum. Evol. 29, 515–547. https://doi.org/10.1006/jhev.1995.1074.
Martínez-Monzón, A., Sánchez-Bandera, C., Fagoaga, A., Oms, O., Agustí, J., Barsky, D., Solano-García, J., Jiménez-Arenas, J.M., Blain, H.A., 2021. Amphibian body size and species richness as a proxy for primary productivity and climate: the Orce wetlands (Early Pleistocene, Guadix-Baza Basin, SE Spain). Palaeogeogr. Palaeoclimatol. Palaeoecol. 110752. https://doi.org/10.1016/J.PALAEO.2021.110752.
Martínez-Navarro, B., Palmqvist, P., Madurell-Malapiera, J., Ros-Montoya, S., Espigares, M.P., Torregrosa, V., Pérez-Claros, J.A., 2010. La fauna de grandes mamíferos de Fuente Nueva 3 y Barranco León 5 – estado de la Cuestión. In: Martínez-Navarro: Ocupaciones Humanas en el Pleistoceno Inferior y Medio de la Cuenca de Guadix-Baza. Junta de Andalucía, Consejería de Cultura, pp. 197–236.
Maté-González, M.A., Aramendi, J., Yravedra, J., González-Aguilera, D., 2017. Statistical comparison between low-cost methods for 3D characterization of cut-marks on bones. Rem. Sens. 9 (9), 873. https://doi.org/10.3390/rs9090873.
Mattson, D.J., 1997. Use of ungulates by Yellowstone grizzly bears. Biol. Conserv. 81, 161–177. https://doi.org/10.1016/S0006-3207(96)00142-5.
Medin, T., Martínez-Navarro, B., Rivals, F., Madurell-Malapeira, J., Ros-Montoya, S., Espigares, M.P., Figueirido, B., Rook, L., Palmqvist, P., 2017. Late Villafranchian *Ursus etruscus* and other large carnivorans from the Orce sites (Guadix-Baza basin, Andalusia, Southern Spain): taxonomy, biochronology, paleobiology, and ecogeographical context. Quat. Int. 431, 20–41. https://doi.org/10.1016/j.quaint.2015.10.053.
Mills, M.G.L., 1984a. Prey selection and feeding habits of the large carnivores in the Southern Kalahari. Kuedue (suppl.) 21, 281–294. https://doi.org/10.4102/koedoe.v27i2.586.
Mills, M.G.L., 1984b. The comparative behavioural ecology of the brown hyaena *Hyaena brunnea* and the spotted hyaena *Crocuta crocuta* in the Southern Kalahari. Koedoe 27, 237–247. https://doi.org/10.4102/koedoe.v27i2.583.
Moclán, A., Domínguez-Rodrigo, M., Yravedra, J., 2019. Classifying agency in bone breakage: an experimental analysis of fracture planes to differentiate between hominin and carnivore dynamic and static loading using machine learning (ML) algorithms. Archaeol. Anthropol. Sci. 11, 4663–4680. https://doi.org/10.1007/s12520-019-00815-6.
Mora, R., Aramendi, J., Courtenay, L.A., González-Aguilera, D., Yravedra, J., Maté-González, M.Á., Prieto-Herráez, D., Vázquez-Rodríguez, J.M., Barja, I., 2022. *Ikhnos*: a novel software to register and analyze bone surface modiufications based on three-dimensional documentation. Animals 12 (20), 2861. https://doi.org/10.3390/ani12202861.
Oms, O., Pares, J.M., Martínez-Navarro, B., Agustí, J., Toro, I., Martínez-Fernandez, G., Turq, A., 2000. Early human occupation of Western Europe: paleomagnetic dates for two paleolithic sites in Spain. P. Natl. Acad. Sci. USA 97, 10666–10670. https://doi.org/10.1073/pnas.180319797.
Oms, O., Anadón, P., Agustí, J., Julià, R., 2011. Geology and chronology of the continental Pleistocene archeological and mammal sites of the Orce area (Baza Basin, Spain). Quat. Int. 243, 33–43. https://doi.org/10.1016/j.quaint.2011.03.048.
Pagès, J., 2004. Analyse factorielle de Données mixtes. Rev. Stat. Appl. 4, 93–111.
Palmqvist, P., Arribas, A., Gröcke, D.R., 2002. The early Pleistocene locality at Venta Micena (Orce, Guadix-Baza Basin, southeast Spain): remarks on the taphonomy, biogeochemistry and paleoecology of the large mammals assemblage. Plioicenica 2, 126–150.
Palmqvist, P., Arribas, A., Martínez-Navarro, B., 2007a. Ecomorphological study of large canids from the lower Pleistocene of southeastern Spain. Lethaia 32 (1), 75–88. https://doi.org/10.1111/j.1502-3931.1999.tb00583.x.
Palmqvist, P., Torregrosa, V., Pérez-Claros, J.A., Martínez-Navarro, B., Turner, A., 2007b. A re-evaluation of the diversity of *Megantereon* (Mammalia, Carnivora, Machairodontinae) and the problem of species identification in extinct carnivores. J. Vertebr. Paleontol. 27 (1), 160–175. https://doi.org/10.1671/0272-4634(2007)27[160:AROTDO]2.0.CO;2.
Palmqvist, P., Pérez-Claros, J.A., Janis, C.M., Gröcke, D.R., 2008. Tracing the ecophysiology of ungulates and predator–prey relationships in an early Pleistocene large mammal community. Palaeogeogr. Palaeoclimatol. Palaeoecol. 266 (1–2), 95–111. https://doi.org/10.1016/j.palaeo.2008.03.015.
Palmqvist, P., Martínez-Navarro, B., Pérez-Claros, J.A., Torregrosa, V., Figueirido, B., Jiménez-Arenas, J.M., Espigares, M.P., Ros-Montoya, S., De Renzi, M., 2011. The giant hyena *Pachycrocuta brevirostris*: modelling the bone-cracking behavior of an extinct carnivore. Quat. Int. 243 (1), 61–79. https://doi.org/10.1016/j.quaint.2010.12.035.
Parkinson, J.A., 2018. Revisiting the hunting-versus-scavenging debate at FLK-Zinj: a GIS spatial analysis of bone modifications produced by hominins and carnivores in the FLK 22 assemblage, Olduvai Gorge, Tanzania. Palaeogeogr. Palaeoclimatol. Palaeoecol. 511, 29–51.
Parkinson, J.A., Plummer, T.W., Bose, R., 2014. A GIS-based approach to documenting large canid damage to bones. Palaeogeogr. Palaeoclimatol. Palaeoecol. 409, 57–71.
Parkinson, J.A., Plummer, T.W., Harston-Rose, A., 2015. Characeterizing felid tooth marking and gross bone damage patterns using GIS image analysis: an experimental feeding study with large felids. J. Hum. Evol. 80, 114–134.
Parkinson, J.A., Plummer, T.W., Oliver, J.S., Bishop, L.C., 2022. Meat on the menu: GIS spatial distribution analysis of bone surface damage indicates that Oldowan hominins at Kanjera South, Kenya, had early access to carcasses. Quat. Sci. Rev. 277, 107314.
Périquet, S., Fritz, H., Revilla, E., 2015. The lion king and the hyaena queen: large carnivore interactions and coexistence. Biol. Rev. 90 (4), 1197–1214.
Pickering, T.R., Egeland, C.P., 2006. Experimental patterns of hammerstone percussion damage on bones: implications for inferences of carcass processing by humans. J. Archaeol. Sci. 33 (4), 459–469. https://doi.org/10.1016/j.jas.2005.09.001.
Pineda, A., Saladié, P., Huguet, R., Cáceres, I., Rosas, A., García-Tabernero, A., Estalrrich, A., Mosquera, M., Ollé, A., Vallverdú, J., 2015. Coexistence among large predators during the lower paleolithic at the site of La mina (Barranc de la Boella, tarragona, Spain). Quat. Int. 388, 177–187.
Pineda, A., Saladié, P., Huguet, R., Cáceres, I., Rosas, A., Estalrrich, A., García-Tabernero, A., Vallverdú, J., 2017. Changing competition dynamics among predators at the late Early Pleistocene site Barranc de la Boella (Tarragona, Spain). Paleogeog. Palaeoclimat. Palaeoecol. 477, 10–26.
Rahimi, A., Recht, B., 2007. Random features for large-scale kernel machines. In: Proceedings of the International Conference of Neural Information Processing Systems, 20, pp. 1–8. https://doi.org/10.5555/2981562.2981710.

Rhodes, R., Rhodes, G., 2004. Prey selection and use of natural and man-made barriers by African wild dogs while hunting. S. Afr. J. Wildl. Res. 34, 135–142.
Rodríguez, J., Rodríguez-Gómez, G., Martín-González, J.A., Goikoetxea, I., Mateos, A., 2012. Predator–prey relationships and the role of *Homo* in Early Pleistocene food webs in Southern Europe. Palaeogeogr. Palaeoclimatol. Palaeoecol. 365–366, 99–114. https://doi.org/10.1016/j.palaeo.2012.09.017.
Rodríguez-Gómez, G., Palmqvist, P., Rodríguez, J., Mateos, A., Martín-González, J.A., Espigares, M.P., Ros-Montoya, S., Martínez-Navarro, B., 2016. On the ecological context of the earliest human settlements in Europe: resource availability and competition intensity in the carnivore guild of Barranco León-D and Fuente Nueva-3 (Orce, Baza Basin, SE Spain). Quat. Sci. Rev. 143, 69–83. https://doi.org/10.1016/j.quascirev.2016.05.018.
Rodríguez-Martín, M., Rodríguez-González, P., Ruiz de Oña Crespo, E., González-Aguilera, D., 2019. Validation of portable mobile mapping system for inspection tasks in thermal and fluid-mechanical facilities. Rem. Sens. 11 (19), 2205. https://doi.org/10.3390/rs11192205.
Rohlf, F.J., 1998. On applications of geometric morphometrics to studies of ontogeny and phylogeny. Syst. Biol. 47, 147–158. https://doi.org/10.1080/106351598261094.
Rohlf, F.K., 1999. Shape statistics: Procrustes superimpositions and tangent spaces. J. Classif. 16, 197–223. https://doi.org/10.1007/s003579900054.
Ros-Montoya, S., Bartolini-Lucenti, S., Espigares, M.P., Palmqvist, P., Martínez-Navarro, B., 2021. First review of lyncodontini material (Mustelidae, carnivora, mammalia) from the lower Pleistocene archaeo-palaeontological sites of Orce (southeastern Spain). Riv. Ital. Paleontol. Stratigr. 127, 33–47.
Saarinen, J., Oksanen, O., Žliobaitė, I., Fortelius, M., DeMiguel, D., Azanza, B., Bocherens, H., Luzón, C., Solano-Garcí, J., Yravedra, J., Courtenay, L.A., Blain, H.A., Sánchez-Bandera, C., Serrano-Ramos, A., Rodríguez-Alba, J.J., Viranta, S., Barsky, D., Tallavaara, M., Oms, O., Agustí, J., Ochando, J., Carrión, J.S., Jiménez-Arenas, J.M., 2021. Pliocene to Middle Pleistocene climate history in the Guadix-Baza Basin, and the environmental conditions of early *Homo* dispersal in Europe. Quat. Sci. Rev. 268, 107132. https://doi.org/10.1016/j.quascirev.2021.107132.
Saladié, P., Rodríguez-Hidalgo, A., Huguet, R., Cáceres, I., Díez, C., Vallverdú, J., Canals, A., Soto, M., Santander, B., Bermúdez de Castro, J.M., Arsuaga, J.L., Carbonell, E., 2014. The role of carnivorans and their relationship to hominin stellements in the TD6-2 level from Gran Dolina (Sierra de Atapuerca, Spain). Quat. Sci. Rev. 93, 47–66.
Sánchez-Bandera, C., Oms, O., Blain, H.-A., Lozano-Fernández, I., Bisbal-Chinesta, J.F., Agustí, J., Saarinen, J., Fortelius, M., Titton, S., Serrano-Ramos, A., Luzón, C., Solano-García, J., Barsky, D., Jiménez-Arenas, J.M., 2020. New stratigraphically constrained palaeoenvironmental reconstructions for the first human settlement in western Europe: the early Pleistocene herpetofaunal assemblages from Barranco León and Fuente Nueva 3 (Granada, SE Spain). Quat. Sci. Rev. 243, 106466. https://doi.org/10.1016/j.quascirev.2020.106466.
Shahriari, B., Swersky, K., Wang, Z., Adams, R.P., Freitas, N., 2016. Taking the human out of the loop: a review of Bayesian optimization. Proc. IEEE 104 (1), 148–175. https://doi.org/10.1109/JPROC.2015.2494218.
Snoek, J., Larochelle, H., Adams, R.P., 2012. Practical Bayesian optimization of machine learning algorithms. Proc. Int. Conf. Neur. Inf. Process. Syst. 25, 2951–2959.
Sokal, R.R., Rohlf, F.J., 1981. Biometry: the Principles and Practice of Statistics in Biological Research. Freeman, New York.
Tancik, M., Srinivasan, P., Milenhall, B., Fridovich-Keil, S., Raghavan, N., Singhal, U., Ramamoorthi, R., Barron, J.T., Ng, R., 2020. Fourier features let networks learn high frequency functions in low dimensional domains. Proc. Int. Conf. Neur. Inf. Process. Syst. arXiv: 2006.10739v1.
Tappen, M., Lordkipanidze, D., Bukshianidze, M., Ferring, R., Vekua, A., 2007. Are you in or out (of Africa)? Site formation at Dmanisi and actualistic studies in Africa. In: Pickering, T.R., Schick, K., Toth, N. (Eds.), Breathing Life into Fossils: Taphonomic Studies in Honor of C.K. Brain. Bloomington. Stone Age Institution Press, pp. 119–135.
Tappen, M., Bukhsianidez, M., Ferring, R., Coil, R., Lordkipanidze, D., 2022. Life and death at Dmanisi, Georgia: taphonomic signals from the fossil mammals. J. Hum. Evol. 171, 103249. https://doi.org/10.1016/j.jhevol.2022.103249.
Tilson, R.L., Henschel, J.R., 1986. Spatial arrangement of spotted hyaena groups in a desert environment, Namibia. Afr. J. Ecol. 24 (3), 173–180. https://doi.org/10.1111/j.1365-2028.1986.tb00358.x.
Titton, S., Barsky, D., Bargallo, A., Vergès, J.M., Guardiola, M., Solano, J.G., Jimenez Arenas, J.M., Toro-Moyano, I., Sala-Ramos, R., 2018. Active percussion tools from the Oldowan site of Barranco León (Orce, Andalusia, Spain): the fundamental role of pounding activities in hominin lifeways. J. Archaeol. Sci. 96, 131–147. https://doi.org/10.1016/j.jas.2018.06.004.
Titton, S., Barsky, D., Bargalló, A., Serrano-Ramos, A., Vergès, J.M., Toro-Moyano, I., Sala-Ramos, R., García-Solano, J.G., Jimenez Arenas, J.M., 2020. Subspheroids in the lithic assemblage of Barranco León (Spain): recognizing the late oldowan in Europe. PLoS One 15 (1), e0228290. https://doi.org/10.1371/journal.pone.0228290.
Titton, S., Oms, O., Barsky, D., Bargalló, A., Serrano-Ramos, A., García-Solano, J., Sánchez-Bandera, C., Yravedra, J., Blain, H.-A., Toro-Moyano, I., Jiménez Arenas, J.M., Sala-Ramos, R., 2021. Oldowan stone knapping and percussive activities on a raw material reservoir deposit 1.4 million years ago at Barranco León (Orce, Spain). Archaeol. Anthropol. Sci. 13, 108. https://doi.org/10.1007/s12520-021-01353-w.
Toro-Moyano, I., Lumley, H. de, Fajardo, B., Barsky, D., Celiberti, V., Grégoire, S., Martínez-Navarro, B., Espigares, M.P., Ros-Montoya, S., 2009. L'industrie lithique des gisements du Pléistocène inférieur de Barranco León et Fuente Nueva 3, Granade, Espagne. L'Anthropologie 113, 111–124. https://doi.org/10.1016/j.anthro.2009.01.006.
Toro-Moyano, I., Martínez-Navarro, B., Agustí, J., 2010. Ocupaciones Humanas en el Pleistoceno inferior y medio de la cuenca de Guadix-Baza. Memoria Científica. Junta de Andalucía, Consejería de Cultura. EPG Arqueología Monografias.
Toro-Moyano, I., Barsky, D., Cauche, D., Celiberti, V., Grégoire, S., Lebegue, F., Moncel, M.H., Lumley, H., 2011. The archaic stone-tool industry from Barranco León and Fuente Nueva 3, (Orce, Spain): evidence of the earliest hominin presence in southern Europe. Quat. Int. 243, 80–91. https://doi.org/10.1016/j.quaint.2010.12.011.
Toro-Moyano, I., Martínez-Navarro, B., Agustí, J., Souday, C., Bermúdez de Castro, J.M., Martinón-Torres, M., Fajardo, B., Duval, M., Falguères, C., Oms, O., Parés, J.M., Anadón, P., Julià, R., García-Aguilar, J.M., Moigne, A.M., Espigares, M.P., Ros-Montoya, S., Palmqvist, P., 2013. The oldest human fossil in Europe, from Orce (Spain). J. Hum. Evol. 65, 1–9. https://doi.org/10.1016/j.jhevol.2013.01.012.
Turner, A., 1992. Large carnivores and earliest European hominids: changing determinants of resource availability during the Lower and Middle Pleistocene. J. Hum. Evol. 22 (2), 109–126. https://doi.org/10.1016/0047-2484(92)90033-6.
Turner, A., 1995. The Villafanchian large carnivore guild: geographic distribution and structural evolution. Il Quat. 8, 349–356.
Turner, A., Antón, M., 1996. The giant hyaena, *Pachycrocuta brevirostris* (mammalia, carnivora, Hyaenidae). Geobios 29 (4), 455–468. https://doi.org/10.1016/S0016-6995(96)80005-2.
Turner, A., Antón, M., 1997. The Big Cats and Their Fossil Relatives. Columbia University Press, New York.
Turq, A., Martínez Navarro, B., Palmqvist, P., Arribas, A., Agustí, J., Rodríguez Vidal, J., 1996. Le Plio-Pléistocène de la région d'Orce, province de Grenade, Espagne : bilan et perspectives de recherche. Paléo 8, 161–204.
Valtierra, N., Courtenay, L.A., López-Polín, L., 2020. Microscopic analyses of the effects of mechanical cleaning interventions on cut marks. Archaeological and Anthropological Sciences 12, 193. https://doi.org/10.1007/s12520-020-01153-8.
Vezina, A.F., 1985. Empirical Relationships between predator and prey size among terrestrial vertebrate predators. Oecologia (Berl.) 67 (4), 555–565. https://doi.org/10.1007/BF00790027.
Villa, P., Mahieu, E., 1991. Breakage patterns of human long bones. J. Hum. Evol. 21, 27–48. https://doi.org/10.1016/0047-2484(91)90034-S.
Wasserstein, R.L., Schirm, A.L., Lazar, N.A., 2019. Moving to a world beyond "p < 0.05". Am. Statistician 73, 1–19. https://doi.org/10.1080/00031305.2019.1583913.
Wiering, M.A., van der Ree, M.H., Embreschts, M.J., Stollenga, M.F., Meijster, A., Nolte, A., Schomaker, L. R. B Schomaker, 2013. The neural support vector machine. In: The 25th Benelux Artificial Intelligence Conference, 257–254.
Yravedra, J., 2005. Tafonomía Aplicada a Zooarqueología. Lerko Print, Madrid.
Yravedra, J., Lagos, L., Bárcena, F., 2011. A taphonomic study of wild wolf (*Canis lupus*) modification of horse bones in northwestern Spain. J. Taphonomy. 9, 37–65.
Yravedra, J., Andrés, M., Domínguez-Rodrigo, M., 2013. A taphonomic study of the African wild dog (*Lycaon pictus*). Archaeological and Anthropological Sciences 6 (2), 113–124. https://doi.org/10.1007/s12520-013-0164-1.
Yravedra, J., Maté-González, M.Á., Courtenay, L.A., González-Aguilera, D., Fernández, M.F., 2019. The use of canid tooth marks on bone for the identification of livestock predation. Sci. Rep. 9 (1). https://doi.org/10.1038/s41598-019-52807-0.
Yravedra, J., Solano, J.A., Courtenay, L.A., Saarinen, J., Linares-Matás, G., Luzón, C., Serrano-Ramos, A., Herranz-Rodrigo, D., Cámara, J.M., Ruiz, A., Titton, S., Rodríguez-Alba, J.J., Mielgo, C., Blain, H.A., Agustí, J., Sánchez-Bandera, C., Montilla, E., Toro-Moyano, I., Fortelius, M., Oms, O., Barsky, D., Jiménez-Arenas, J.M., 2021. Use of meat resources in the early Pleistocene assemblages from Fuente Nueva 3 (Orce, Granada, Spain). Archaeol. Anthropol. Sci. 13, 213. https://doi.org/10.1007/s12520-021-01461-7.
Yravedra, J., Solano, J.A., Herranz-Rodrigo, D., Linares-Matás, G.J., Saarinen, J., Rodríguez-Alba, J.J., Titton, S., Serrano-Ramos, A., Courtenay, L.A., Mielgo, C., Luzón, C., Cámara, J., Sánchez-Bandera, C., Montilla, E., Toro-Moyano, I., Barsky, D., Fortelius, M., Agusti, J., Blain, A.H., Oms, O., Jiménez-Arenas, J.M., 2022a. Unraveling hominin activities in the zooarchaeological assemblage of Barranco León (Orce, Granada, Spain). J. Palaeolithic Archaeol. 5, 6. https://doi.org/10.1007/s41982-022-00111-1.
Yravedra, J., Courtenay, L.A., Herranz-Rodrigo, D., Rodríguez-Alba, J.J., Linares-Matás, G., Estaca-Gómez, V., Luzón, C., Serrano-Ramos, A., Maté-González, M.Á., Solano, J.A., González-Aguilera, D., Jiménez-Arenas, J.M., 2022b. Taphonomic characterisation of extinct eurasion carnivores through geometric morphometrics. Sci. Bull. 67 (16), 1644–1648.